Title

Loss of Sip1 leads to migration defects and retention of ectodermal markers during lens development

Journal

Cells and Development, 131(1)

ISSN

2667-2901

Authors

Manthey, Abby L

Lachke, Salil A

FitzGerald, Paul G

et al.

Publication Date

2014-02-01

DOI

10.1016/j.mod.2013.09.005

Peer reviewed

Published in final edited form as:
Mech Dev. 2014 February ; 131: 86–110. doi:10.1016/j.mod.2013.09.005.

Loss of Sip1 leads to migration defects and retention of ectodermal markers during lens development

Abby L. Manthey[a], **Salil A. Lachke**[a,b], **Paul G. FitzGerald**[c], **Robert W. Mason**[d], **David A. Scheiblin**[a], **John H. McDonald**[a], and **Melinda K. Duncan**[a,*]

[a]Department of Biological Sciences, University of Delaware, Newark, DE 19716, USA

[b]Center for Bioinformatics and Computational Biology, University of Delaware, Newark, DE 19716, USA

[c]Department of Cell Biology and Human Anatomy, School of Medicine, University of California, Davis, CA 95616, USA

[d]Department of Biomedical Research, Alfred I duPont Hospital for Children, Wilmington, DE 19803, USA

Abstract

SIP1 encodes a DNA-binding transcription factor that regulates multiple developmental processes, as highlighted by the pleiotropic defects observed in Mowat-Wilson Syndrome, which results from mutations in this gene. Further, in adults, dysregulated SIP1 expression has been implicated in both cancer and fibrotic diseases, where it functionally links TGFβ signaling to the loss of epithelial cell characteristics and gene expression. In the ocular lens, an epithelial tissue important for vision, Sip1 is co-expressed with epithelial markers, such as E-cadherin, and is required for the complete separation of the lens vesicle from the head ectoderm during early ocular morphogenesis. However, the function of Sip1 after early lens morphogenesis is still unknown. Here, we conditionally deleted *Sip1* from the developing mouse lens shortly after lens vesicle closure, leading to defects in coordinated fiber cell tip migration, defective suture formation, and cataract. Interestingly, RNA-Sequencing analysis on *Sip1* knockout lenses identified 190 differentially expressed genes, all of which are distinct from previously described Sip1 target genes. Furthermore, 34% of the genes with increased expression in the *Sip1* knockout lenses are normally downregulated as the lens transitions from the lens vesicle to early lens, while 49% of the genes with decreased expression in the *Sip1* knockout lenses are normally upregulated during early lens development. Overall, these data imply that Sip1 plays a major role in reprogramming the lens vesicle away from a surface ectoderm cell fate towards that necessary for the development of a transparent lens and demonstrate that Sip1 regulates distinctly different sets of genes in different cellular contexts.

*To whom all correspondence should be addressed: Department of Biological Sciences, 327 Wolf Hall, University of Delaware, Newark, DE 19716, Tel.: 302-831-0533, Fax.: 302-831-2281, duncanm@udel.edu.

Keywords

Sip1; Zeb2; lens development; ectodermal cell fate

1. Introduction

The ZEB transcription factors – Smad interacting protein 1 (Sip1, ZEB2) and δ-crystallin enhancer binding factor 1 (δEF1, ZEB1) – are characterized by their centrally located homeodomain and two separate clusters of DNA binding zinc-fingers at the N-terminus and C-terminus (Verschueren et al., 1999; van Grunsven et al., 2001; Nelles et al., 2003; Vandewalle et al., 2009; Grabitz and Duncan, 2012). Both Sip1 and δEF1 directly bind to 5′-CACCT(G) sequences (found in E2 box elements) with both zinc-finger hands, thus competing with basic helix-loop-helix activators for these sites (Sekido et al., 1994; Remacle et al., 1999; Verschueren et al., 1999). The vast majority of research concerning this gene family focuses on its involvement in epithelial-to-mesenchymal transition (EMT) occurring during wound healing, cancer progression, and fibrosis (Vandewalle et al., 2009).

During EMT, ZEB proteins repress the expression of E-cadherin, P-cadherin, Claudin 4, Connexin 26, and other epithelial specific genes (Vandewalle et al., 2005; Bindels et al., 2006; Vandewalle et al., 2009; Xia et al., 2009). In contrast, Fibronectin, Vimentin, N-cadherin, and other mesenchymal genes are upregulated by the overexpression or induction of ZEB protein expression. The transcriptional changes mediated by the ZEB proteins in this context occur through both direct binding to gene promoters, and indirect mechanisms. The myriad of downstream genes controlled by Sip1 contribute to the cytoskeletal changes and increased cell motility that are characteristic of EMT, making Sip1 a critical regulator of this process. However, it is not clear if the functional consequence of altered ZEB expression in pathological situations reflects the entire functional repertoire of these proteins during normal embryonic development. This is particularly relevant for tissues that do not utilize EMT as a means of cellular remodeling during development.

During mammalian embryonic development, Sip1 is first expressed in the gastrula (E8), primarily being detected in the early neural plate, neural crest, and paraxial mesoderm (Espinosa-Parrilla et al., 2002; Van de Putte et al., 2003). Homozygous germ line loss of Sip1 protein function leads to a lack of neural tube closure and neural crest migration leading to death by E9.5 in the mouse (Van de Putte et al., 2003). Conditional deletion of *Sip1* in mice later in development has revealed important roles for Sip1 in the development of hematopoetic stem cells, motor neurons, oligodendrocytes, neocortical neurons, the hippocampus, and pain transmission by dorsal root ganglia neurons (Seuntjens et al., 2009; Jeub et al., 2011; Goossens et al., 2011; Weng et al., 2012; Miquelajauregui et al., 2007). Notably, while heterozygous *Sip1* null mice appear normal, heterozygous mutations in the human *SIP1* gene result in Mowat-Wilson Syndrome, a pleiotropic developmental disorder typified by mental retardation coupled to diverse developmental defects with variable penetrance including a lack of intestinal innervation (Hirschsprung's disease), heart malformations, urogenital defects, and eye defects, including micropthalmia and cataract (Garavelli et al., 2003; Mowat et al., 2003; Bassez et al., 2004; Adam et al., 2006; Garavelli and Mainardi, 2007; Ariss et al., 2012; Zweier et al., 2005).

Consistent with the eye defects seen in Mowat-Wilson Syndrome patients, *Sip1* mRNA is detected in the lens at E9.5, shortly after lens induction (Yoshimoto et al., 2005), and continues in all the cells of the lens vesicle, becoming localized mainly to the lens epithelium and young fiber cells as the lens matures. In adult mice, Sip1 protein is detected in both the peripheral lens epithelium and cortical fibers as well as in the inner nuclear layer and occasional ganglion cells in the adult retina (Grabitz and Duncan, 2012). Notably, while the lens does not undergo EMT during normal development, conditional deletion of the *Sip1* gene when the early lens is specified from the head ectoderm results in primary defects in lens vesicle closure associated with defects in FoxE3 expression and subsequent defects in fiber cell differentiation (Yoshimoto et al., 2005). However, it is unclear from these data if the fiber cell differentiation defects are secondary to the lack of vesicle closure and if Sip1 has distinct regulatory roles in these two separate events. Further, how the requirement for Sip1 in lens development relates to its function in other developmental contexts or in diverse pathologies, including cancer, also remain elusive. Here, we delete *Sip1* from the lens shortly after lens vesicle closure, and find that Sip1 regulates multiple genes that are generally distinct from those regulated by Sip1 during cancer and fibrosis, including those whose expression is prominent in the early head ectoderm as well as the corneal epithelium, conjunctiva, and epidermis later in development. This implies that Sip1 is a multi-faceted transcription factor that utilizes specific cues to regulate its function in different cellular contexts.

2. Results

2.1. Sip1 protein is expressed in the developing lens epithelium

Sip1 mRNA is expressed in the mouse lens placode starting at E9.5 with maintained lens expression until E13.5 (Yoshimoto et al., 2005), and we have shown that Sip1 protein is expressed in the lens epithelium and transition zone of adult mice (Grabitz and Duncan, 2012). Here, we show that that Sip1 protein is not detectable by immunostaining in the lens placode at E9.5 (Fig. 1A), but becomes easily detectable in the posterior aspect of the lens vesicle at E10.5 in cells fated to become primary lens fiber cells (Fig. 1B). As the lens vesicle matures, Sip1 is lost in the most central lens fiber cells beginning at E12.5 (Fig. 1C) and becomes uniformly expressed in the lens epithelium by E14.5 (Fig. 1D). By E16.5, however, Sip1 protein is no longer found in the central epithelium, but is maintained in the peripheral epithelium (Fig. 1E). Restriction of Sip1 expression to this region of the epithelium continues in later post-natal time points (Fig. 1F). In the adult, Sip1 remains localized in the peripheral epithelium and cortical fibers (Fig. 1G, H), with lower levels found in the central epithelium (Fig. 1I).

2.2. Deletion of Sip1 in the lens results in cataract formation and abnormalities in fiber cell organization due to early defects in coordinated cell migration

In order to clarify the function of Sip1 in lens fiber cell differentiation, we used a previously described conditional allele (Fig. 2A) (Higashi et al., 2002) to remove *Sip1* from the developing lens using MLR10 Cre, which is first active in the lens vesicle at E10.5 (Zhao et al., 2004). PCR analysis confirmed that *Sip1* exon 7 was not detectable in adult lens DNA

(Fig. 2B) and immunohistochemistry showed that Sip1 protein expression was significantly reduced by E10.5 (Fig. 2D).

In the adult, *Sip1* cKO lenses are opaque (Fig. 3A, B) and dark field analysis shows profound defects in lens shape and size (Fig. 3C, D). The fiber cell structure of these lenses is abnormal (Fig. 3E, F) with major disruptions in the actin cytoskeleton (Fig. 3G, H). Sip1 is expressed primarily in the transition zone of lenses after E12.5, while the major defect in the adult lens appears to be in the lens fiber cells. Consistent with this Sip1 expression domain, the meridional rows, which are formed in the peripheral epithelium as lens epithelial cells transition to lens fibers (Fig. 3I) (Bassnett, 2005), were disorganized in *Sip1* cKO lenses (Fig. 3J) which can be expected to disrupt fiber cell arrangement. The latter was confirmed by scanning electron microscopy (SEM) showing that *Sip1* cKO fiber cells (Fig. 3L) have abnormal fiber cell packing compared to the wild type (Fig. 3K) and also have disorganized membrane protrusions (Fig. 3M, N), that would be expected to greatly compromise lens transparency.

Although loss of Sip1 protein is obvious by E10.5, no major morphological abnormalities are obvious at E12.5 (Fig. 4A, D) or E14.5 (Fig. 4B, E). However, by E16.5, it is apparent that the tips of *Sip1* cKO lens fiber cells fail to migrate towards the optical axis to form the sutures (Fig. 4C, F). These defects in fiber cell curvature and morphology were further highlighted with toluidine-blue staining (Fig. 4G, H, K, L). Importantly, this defect does not appear to be caused by defects in actin assembly, as F-actin is still detected in the lens fiber cells (Fig. 4I, M) and Nap1 (Nck-associated protein 1), a player in actin polymerization during fiber cell migration (Steffen et al., 2004; Rakeman and Anderson, 2006; Maddala et al., 2011), is also found at normal expression levels (Fig. 4J, N and Supplemental Data 1). However, both proteins appear to be partially mislocalized.

2.3. Early fiber cell differentiation markers are unchanged when Sip1 is lost after lens vesicle closure

Yoshimoto et al. (2005) previously showed that the expression of β- and γ-crystallins is downregulated when Sip1 is deleted in the lens placode, implying that Sip1 regulates the fiber differentiation pathway controlling crystallin expression. However, when Sip1 is deleted after lens vesicle closure, the global expression of crystallins is unaffected at E16.5 (Fig. 5A) and β- and γ-crystallin localization is also qualitatively normal (Fig. 5B – E). Further, the expression of Aquaporin 0, a major component of lens fiber cell membranes (Fig. 5F), is upregulated as expected as fiber cells begin to differentiate (Fig. 5G). The apparent mislocalization is likely due to the morphological defects seen in these lenses (Fig. 3). Even in adult lenses, there were no qualitative changes in crystallin expression in the *Sip1* cKO lens detected by SDS-PAGE (Supplemental Data 2) and although quantitative two dimensional (2D) DIGE analysis showed that some members of the γ-crystallin family and a few cytoskeletal proteins are altered in the adult, the differences were all less than two fold (Supplemental Table 3). The proteome of adult *Sip1* cKO lenses also exhibited many new protein species that were all identified as crystallins, probably due to the extensive post-translational modifications that are typically observed in both cataractous and aging lenses (Ponce et al., 2006; Robertson et al., 2008; Wilmarth et al., 2006; Ueda et al., 2002;

Jimenez-Asensio et al., 1999). Thus, these changes in fiber cell proteins are unlikely related to the primary function of Sip1.

The expression levels of other lens fiber cell markers, such as Prox1 and c-Maf, are also unaffected in the adult *Sip1* cKO lens, suggesting that Sip1 does not regulate lens fiber cell differentiation per se, although c-Maf expression was found to be slightly reduced at E16.5 (Supplemental Data 3), indicating a delay in expression. It was previously reported that FoxE3, a gene necessary for lens vesicle closure and maintenance and proliferation of the lens epithelium, is downregulated in lenses with *Sip1* deletion at the lens placode stage and it was proposed that *FoxE3* is a direct Sip1 target gene (Yoshimoto et al., 2005). However, in lenses from our conditional knockout mice, *FoxE3* mRNA levels are not significantly altered (Fig. 6A) and protein expression remains similar to that of the wild type controls (Fig. 6B, C).

As we found no evidence of changes in fiber cell differentiation marker expression, FoxE3, or markers of lens epithelial cell proliferation and apoptosis (data not shown) in our *Sip1* mutant lenses, we expanded our investigation to look for alterations in the expression of other known Sip1 target genes.

2.4. Known Sip1 target genes, validated in EMT and cancer, are unchanged in the Sip1 conditional knockout lens

In pathological situations such as epithelial-to-mesenchymal transition (EMT) in cancer, ZEB proteins, including Sip1, are known to repress the expression of epithelial markers such as E-cadherin and activate the expression of mesenchymal markers such as Vimentin and N-cadherin (Vandewalle et al., 2005; Bindels et al., 2006; Vandewalle et al., 2009; Xia et al., 2009). These three genes are all expressed in the normal developing lens (Fig. 7A, D, G) (Pontoriero et al., 2009; Xu et al., 2002; Sax et al., 1990). Although E-cadherin levels in the lens epithelium are significantly downregulated in the *Sip1* cKO at E16.5 (Fig. 7B, C), they recover to normal levels in the adult (data not shown). Furthermore, Vimentin, expressed in the epithelium and at low levels in the fiber cells, and N-cadherin, expressed primarily in the lens fiber cells, were not significantly altered in the *Sip1* cKO at E16.5 (Fig. 7E, F, H, I), although some mislocalization is apparent. Additionally, α-smooth muscle actin (αSMA), a commonly used “general” EMT marker, the expression of which has been indirectly linked to Sip1's sister protein δEF1 during EMT (Nishimura et al., 2006), fails to be upregulated in the *Sip1* cKO (Supplemental Data 4), supporting the idea that Sip1 regulates different genes in the developing lens compared to pathological processes leading to fibrosis and cancer.

2.5. Global analysis shows that the mRNA levels for multiple genes are altered in Sip1 conditional knockouts

Since the investigation of candidate genes involved in the *Sip1* knockout lens phenotype was not fruitful, we used RNA-Sequencing to compare the transcriptomes of wild type and *Sip1* cKO lenses at E15.5 (a time point proximal to the onset of the most obvious *Sip1* knockout phenotype) in an attempt to identify the molecular pathways regulated by Sip1 in the maturing lens. This analysis revealed that wild type E15.5 mouse lenses express over 7,700 genes at levels above 2 RPKM (reads per kilobase per million) (GEO accession GSE49949),

but the expression of only 190 genes were changed more than 2.5 fold in the *Sip1* cKO lenses (Table 1).

Similar to the quantitative protein analysis, none of the cancer related EMT genes that are known to be regulated by Sip1 are found to be altered in this analysis or in validation experiments (Table 2). This contrasts with proposed Sip1 targets identified in other systems (Vandewalle et al., 2005; Bindels et al., 2006; Xia et al., 2009; Vandewalle et al., 2009). Further, the RNA-Seq data support our observation that FoxE3 expression was unaltered at the RNA level in *Sip1* cKO lenses (Fig. 6). These data also show that c-Maf RNA levels are downregulated just over 2 fold, supporting our observation that the expression of c-Maf, a transcription factor that regulates fiber cell differentiation, is delayed (Supplemental Data 3).

Further analysis using Ingenuity Pathway Analysis (IPA) (Ingenuity Systems, Inc., www.ingenuity.com), revealed that subsets of the differentially expressed genes are involved in multiple cellular processes, including cancer and the control of cellular morphology and development (Supplemental Data 5). However, although manual searches found that some of the differentially expressed genes have been indirectly linked to Sip1 in the literature, IPA did not identify explicit connections between any of the genes with altered expression and known Sip1 functions. Upon further analysis, we noticed that the list of altered genes included not only genes preferentially expressed in the lens, but also in the corneal epithelium, conjunctiva, and epidermis. Notably, all of these tissues are in close proximity in the adult eye and their precursors have a common origin in the head ectoderm during early development (Graw, 2010).

2.6. Ectodermal/pre-placodal proteins are aberrantly expressed in the Sip1 conditional knockouts

Two genes, Keratin 8 (K8) and one of its binding partners Keratin 18 (K18), were of particular interest as Keratin 8 has recently been identified as a limbal marker in the adult cornea epithelium (Pajoohesh-Ganji et al., 2012). K8 and K18 – increased 48 fold and 7.5 fold, respectively, in the *Sip1* cKOs in the RNA-Seq data – are type II and type I keratin subunits which are able to form a heterodimeric pair known to be expressed in simple epithelia (Moll et al., 1982). The expression of K8/18 lends itself to the hypothesis that Sip1 could be involved in differentiating between the lens and neighboring ectodermal derived tissues. However, very little is known about the function or expression of K8/18 during ocular development.

As expected, K8 is expressed in the limbal region of the adult cornea (Fig. 8A), but is largely absent from the wild type adult lens (Fig. 8B). Interestingly, K8 was found to be highly expressed in the wild type head ectoderm at E9.5, including the region of the lens placode (Fig. 8C). Using qRT-PCR to validate the RNA-Seq, it appears that Keratin 8 is significantly increased 41 fold and Keratin 18 is significantly increased 5 fold (Fig. 8D) in *Sip1* cKO lenses. Further, K8 protein expression is maintained in the lens vesicle of the wild type lens after closure (Fig. 8E), but is greatly downregulated at E12.5 (Fig. 8G) and lost by E14.5 (Fig. 8I, K) although expression is maintained in the embryonic corneal epithelium and conjunctiva. In the *Sip1* cKOs, however, K8 expression is maintained in the lens,

particularly in the primary fiber cells and peripheral epithelium (Fig. 8F, H, J, L), corresponding to where Sip1 is normally expressed (Fig. 1).

Thus, K8 is not being upregulated when Sip1 expression is lost from the lens, but instead fails to be downregulated as the lens is segregating from the surface ectoderm, implying that Sip1 may regulate the decision between lens and head ectoderm/corneal epithelial cell fate. To test this, we performed a global analysis (Table 1) to compare the normal expression levels of the 190 genes differentially expressed at E15.5 between wild type and *Sip1* cKO lenses between E10.5 (lens vesicle stage) and E12.5 (the completion of primary fiber cell elongation) using previously compiled microarray data (Lachke et al., 2012). This period corresponds to the stage of lens development where Sip1 protein expression is upregulated (Fig. 1) and the lens undergoes many changes in gene expression as its undergoes morphogenesis (Lachke et al., 2012).

2.7. Investigating the normal expression pattern of the differentially expressed genes reveals dual functions for Sip1 in the lens

At the 2.5-fold cut-off, the expression levels of 103 genes were identified as increased in the *Sip1* cKO compared to wildtype. Of these genes, 80 were included in the *iSyTE* Affymetrix dataset (Lachke et al., 2012) and are expressed at significant levels in the early lens. Further, 24 of these genes did not change and 21 increased in the lens as it transitions from E10.5 to E12.5. Interestingly, 35 genes (34%) are normally downregulated in the lens as it transitions from E10.5 to E12.5, implying that Sip1 may act as a repressor of these genes during normal lens development. Increased expression of six of the genes was confirmed by qRT-PCR (Table 3), and each contained at least one potential Sip1 binding site within their promoter (Table 4).

At the 2.5-fold cut-off, 87 genes are decreasing in expression in the *Sip1* cKO. Out of these, 60 genes were included in the *iSyTE* Affymetrix dataset (Lachke et al., 2012) and expressed at significant levels in the early lens. 15 of these genes showed no change in expression while only 2 are downregulated as the lens transitions from E10.5 to E12.5. Interestingly, a large portion of these genes (43, 49%) are normally upregulated as the lens transitions from E10.5 to E12.5. Similarly, the promoters of these genes also appear to contain several potential Sip1 binding sites as highlighted by the sites found in the promoter for Trpc6 (Table 4). Thus, although Sip1 is primarily known to be a repressor and may act to repress genes normally expressed in the head ectoderm but not the lens, it appears that it also may activate a number of genes in the developing lens.

3. Discussion

The ocular lens is a specialized tissue composed of an anterior layer of flattened, proliferative epithelial cells, which maintain the lens epithelium and, at the lens equator, also differentiate into lens fiber cells which make up the bulk of the lens mass (Wride, 1996; Piatigorsky, 1981). Morphologically, the lens originates from a section of the surface ectoderm which thickens to form the lens placode during early embryogenesis (Reviewed in Lovicu and McAvoy, 2005). The lens placode then invaginates to form the lens pit and is subsequently able to pinch off from the presumptive corneal epithelium to form a hollow

ball of cells, known as the lens vesicle. The fate of each of these cells acts to give the lens its distinct polarity and transparency.

Like most tissues, the exquisite structure of the lens requires multiple cell signaling pathways and transcriptional modules for its development, while dysregulation of these processes causes eye defects due to the importance of the lens as a signaling center regulating eye development and/or the simple loss of lens transparency, also known as cataract (Cvekl and Duncan, 2007). The timing of gene expression is of utmost importance. It has been established that some transcription factors known to be critical for lens development, most notably Pax6, have distinctly different functions at different times in this process (Cvekl and Piatigorsky, 1996; Grindley et al., 1995; Duncan et al., 1998; Cvekl et al., 1995; Cvekl et al., 2004; Ashery-Padan et al., 2000; Shaham et al., 2009); functions that, if disrupted, will lead to global changes in downstream gene expression (Chauhan et al., 2002; Xie et al., 2013). However, this phenomenon has not been comprehensively investigated for other transcription factors important for lens development.

An earlier study, utilizing Le-Cre to delete Sip1 at the lens placode stage, demonstrated that this gene is important for the separation of the lens vesicle from the presumptive corneal epithelium, a phenomenon associated with reduced levels of FoxE3 expression, a transcription factor known to control this process (Yoshimoto et al., 2005). Here, we show that Sip1 protein levels are undetectable in the lens placode and upregulate as the lens vesicle separates from the head ectoderm, with higher protein levels detected in the posterior lens vesicle which will give rise to lens fibers. While early expression of Sip1 is consistent with the defects seen in lens vesicle closure in this prior study, the present study did not find abnormalities in the expression of FoxE3 when Sip1 is lost after lens vesicle closure, suggesting that Sip1's role in FoxE3 regulation changes during lens development.

Further, while deletion of the Sip1 gene in the lens placode led to defects in fiber cell elongation associated with reduction/loss of expression of classical fiber cell markers such as crystallins, we found that removal of Sip1 at the lens vesicle stage did not affect either primary fiber cell elongation or the expression of these fiber cell markers. We conclude that the lens fiber defects observed in the prior study did not arise due to the primary loss of Sip1 function. It is possible that Sip1 expression as the lens placode transitions to the lens vesicle is necessary to program these cells into a state that is competent to respond appropriately to fiber cell differentiation signals while not regulating the most common markers of fiber cell differentiation directly. This role is further supported by the delayed expression of c-Maf when Sip1 is lost rather than the complete loss of c-Maf protein expression observed in some fiber cell differentiation phenotypes (Zhao et al., 2008; Wang et al., 2010).

While Sip1 does not appear to regulate lens fiber cell differentiation, lens cell survival, or lens cell proliferation after lens vesicle closure, lack of Sip1 from the lens vesicle onward results in defects in the migration of fiber cell tips necessary for the proper packing of lens fiber cells and formation of lens sutures. These primary defects in lens development manifest as severe defects in the adult lens fiber cell morphology and organization of the meridional rows, leading to a loss of lens transparency. These defects do not appear to be either directly or indirectly related to defects in F-actin expression or polymerization, and

the expression levels of Nap1 (a component of the WAVE-2 complex important for actin polymerization and branching involved in fiber cell migration) are generally normal even though mislocalized (Steffen et al., 2004; Rakeman and Anderson, 2006; Maddala et al., 2011; Gautreau et al., 2004). It should be noted that the morphological consequences of Sip1 deletion from the entire lens are ultimately seen in the fiber cells and are likely caused by the loss of early Sip1 expression in the posterior lens vesicle in cells fated to become the primary fiber cells. However, in late embryonic and early postnatal development, Sip1 is largely expressed in the peripheral lens epithelium, and loss of Sip1 in these cells likely augments the initial defect in the fiber cells as the lens epithelium both organizes the meridional rows and provides signals (e.g. planar cell polarity signaling, etc.) that regulate the appropriate migration of lens fiber cells (Bassnett, 2005; Sugiyama and McAvoy, 2012).

In pathological situations such as the EMT-like changes seen in cancer as well as the pathogenesis of fibrosis, Sip1 represses the expression of epithelial specific genes such as E-cadherin while activating the expression of mesenchymal genes such as Vimentin and N-Cadherin (Vandewalle et al., 2005; Bindels et al., 2006; Vandewalle et al., 2009; Xia et al., 2009). However, in the normal lens, E-cadherin is co-expressed in the same cells that exhibit the highest Sip1 protein levels while Vimentin and N-cadherin levels upregulate in the fibers, cells which express lower levels of Sip1 compared to the peripheral epithelium. One of the fundamental questions this work seeks to answer is: Do the consequences of altered Sip1 expression in pathological situations reflect the full function of this protein during normal development of the lens, a tissue that does not utilize EMT during maturation? Notably, Vimentin and N-cadherin expression levels are not altered in Sip1 knockout lenses, implying that Sip1 regulates different target genes in the developing lens than it does in adult pathologies. Consistent with this, E-cadherin, a gene repressed by Sip1 in several cancers, is significantly downregulated in the embryonic lens when Sip1 is lost, but is recovered in the adult, the opposite effect of what would be expected if Sip1 were a repressor of E-cadherin in this tissue. While these candidate gene approaches did not identify any potential Sip1 target genes in the lens, it is apparent that Sip1 is playing a unique role in this tissue compared to its function in pathology.

To identify genes that Sip1 may regulate in lens development, an unbiased, global approach was utilized to compare gene expression in *Sip1* knockout lenses with wild type controls at E15.5. This analysis revealed that 190 genes were differentially expressed in the Sip1 knockout lens, none of which were previously linked to Sip1 gene function. Furthermore, only three of these genes have been identified previously as potential downstream targets of the Zeb family in the literature: Desmoplakin (Dsp) and Keratin 18 (Krt18/K18) are both epithelial cell markers, which are downregulated during EMT concomitant with an increase in the ZEB proteins (Chua et al., 2007), and Phospholemman (Fxyd1), a Na^+ -K^+ -ATPase-interacting regulatory protein found to upregulate simultaneously with a Zeb family member in skeletal muscle of high-fat fed sedentary rats (Galuska et al., 2009). While there is currently no evidence of direct binding of Sip1 to these gene promoters, we have identified three potential Zeb binding sites upstream of the Dsp structural gene and one Zeb binding site upstream of the Krt18 gene (Table 4). However, bioinformatic analysis was unable to demonstrate that these potential Sip1 sites were enriched in the differential expressed genes.

This is likely a result of the short length of the known Sip1 consensus binding site which would thus be common in the genome. Further, the expression of many known Sip1 target genes (i.e. E-cadherin) does not change in the lenses of our Sip1 conditional knockouts. We hypothesize that although Sip1 binding sites are likely common in the genome, Sip1 function is tissue/context specific.

Importantly, when we compared our list of differentially expressed genes with those previously identified as differentially regulated from E10.5 (when Sip1 protein is first detected in the early lens) to E12.5 (when the primary lens fibers are completing their elongation) (Lachke et al., 2012), 35 of the mRNAs that increase in abundance upon Sip1 loss from the lens were found to be normally downregulated as the lens transitions from the lens vesicle to the early lens. Conversely, 43 of the mRNAs that are of lower abundance in the *Sip1* knockout lens normally increase in expression as the lens forms. Although Sip1 has most often been heralded as a repressor, a possible role as a direct transcriptional activator has also been suggested (i.e. activator of *FoxE3* expression) (Yoshimoto et al., 2005). In our analysis, while numerous genes appear to be activated by Sip1 (and thus their mRNAs are found at lower levels when Sip1 is lost), few appear to play known roles in lens development. Notably, several genes of the tubulin family including Tubb2a, Tubb2b, Tubb4 are decreased in the *Sip1* knockout lenses consistent with a prior report that downregulation/disorganization of microtubules is associated with defects in fiber cell migration (Chen et al., 2008).

During the early stages of embryonic development, a pre-placodal cell in the head ectoderm may initially express an large number of genes, but as these cells are further specified and differentiate during the thickening and invagination of the lens placode, they greatly remodel their proteome to express proteins critical for the function of each specific tissue formed, including the epidermis, cornea, conjunctiva, and lens. For the lens, this involves expressing proteins that will initiate the expression of genes important for lens clarity and cell structure while repressing the expression of ectodermal, corneal, and conjunctival genes. In the *Sip1* knockout lens, the retention of numerous uncharacteristic genes increases the likelihood of improper lens development and formation of cataract. For example, Dickkopf 1 (Dkk1) (normally downregulated after lens vesicle closure, but increased 10 fold when Sip1 was lost), is a repressor of the Wnt/β-catenin pathway and has been proposed to play a role in the planar cell polarity pathways responsible for the organization and polarity of numerous ectoderm-derived tissues (Caneparo et al., 2007). Further, changes in the structural and metabolic machinery, including altered expression of Keratin 8/18 (Krt8/18), Troponin T1 (Tnnt1), beta-Tropomyosin (Tpm2), Lengsin (Lgsn), Aldehyde dehydrogenase 1A3 (Aldh1A3), ubiquitin carboxy-terminal hydrolase L1 (Uchl1), and many others, would be expected to further compromise lens transparency by altering the cytoskeletal properties (including actin polymerization and durability) and changing the fine-tuned enzymatic pathways regulating lens homeostasis.

From our data, we hypothesize that Sip1 acts to continually repress the expression of non-lens genes, while also upregulating a number of additional genes. Further, this regulation may occur through indirect changes in SMAD signaling in addition to direct binding, as many of these genes have prospective Zeb binding sites in their upstream promoter region

(Table 4) and additional interactions in the enhancer and 3′-UTR regions of these genes are also possible. However, it is unlikely that just one of the 190 differentially expressed genes is at fault for the major morphological abnormalities found in the *Sip1* cKO, and global or broad range changes in groups of genes may be more useful in explaining the phenotype.

Thus, it would appear that Sip1 is a dual functioning transcription factor, acting on lens vesicle closure genes (i.e. FoxE3) when it is expressed at low levels in the lens placode and anterior lens vesicle early in development, while high level expression of Sip1 later in development acts to not only activate a subset of lens genes, but to also repress ectodermal genes. The primary focus in the literature has been on the function of transcription factors which activate genes important for lens development. To our knowledge, Sip1 is the first reported transcription factor whose function, in part, also appears to be necessary to repress the expression of genes normally found in the head ectoderm during lens development.

Notably, the numerous downstream genes affected when Sip1 is lost in the lens are indicative of the complex nature and phenotype, including prominent facial abnormalities and ocular defects, associated with the human disorder Mowat-Wilson Syndrome caused by heterozygous mutations in the Sip1 gene (McKinsey et al., 2013; Garavelli and Mainardi, 2007; Garavelli et al., 2003; Bassez et al., 2004; Zweier et al., 2005; Ariss et al., 2012). Although this work identifies the phenotypic consequences of the loss of Sip1 from the lens, global changes in gene expression associated with this phenotype, as well as tentative functions, further research is warranted in order to enhance our understanding of the definitive role of Sip1 in the lens environment.

4. Methods

4.1. Animals

Mice which harbor the Sip1 gene with exon seven flanked by LoxP sites (*Sip1*$^{flox(ex7)}$ or *Zeb2*$^{tm1.1Yhi}$ in the Mouse Genome Informatics Database) (Higashi et al., 2002) were obtained from Dr. Yujiro Higashi, (Osaka University, Osaka, Japan). These mice were then mated to *MLR10Cre* mice expressing Cre recombinase in all lens cells from the lens vesicle stage onward (Zhao et al., 2004) which were originally obtained from Dr. Michael Robinson (Miami University, Oxford, Ohio) on an FVB/N genetic background, then backcrossed four generations to C57Bl/6<har> in our laboratory. All mice in this study were bred and maintained in the University of Delaware Animal Facility and adhered to the ARVO Statement for the Use of Animals in Ophthalmic and Vision Research. Embryos were staged by designating the day that the vaginal plug was observed in the dam as E0.5. No lens defects were ever observed in mice either homozygous or heterozygous for either the MLR10Cre transgene or the Sip1 flox allele alone (data not shown).

4.2. DNA Analysis

DNA was isolated from tail biopsies and lenses of adult *Sip1* conditional knockout mice (*Sip1* cKO) and C57Bl/6<har> mice (wild type) using the PureGene Tissues and Mouse Tail kit (Gentra Systems, Minneapolis, MN). Mice were genotyped for the presence of the floxed *Sip1* allele using primers flanking the loxP site in intron 6 (fwd 5′-GAA CTA GTT GAA TTG GTA GAA TCA ATG GGG and rev 5′-GTA AAG GCT CTC TAC GCC TTT TTC

AGT TAG). Mice were also genotyped for the presence of the *MLR10Cre* transgene as previously described (Zhao et al., 2004). The extent of exon seven deletion of the *Sip1* gene in lens cells was determined by PCR analysis of lens DNA using primers for *Sip1* intron six (fwd 5′-GAA CTA GTT GAA TTG GTA GAA TCA ATG GGG) and intron seven (rev 5′-CAC TGC CAC TTT GGC TCC TAT TTT GCA AAC).

4.3. Morphological Analysis and Immunohistochemistry

Animals were euthanized and isolated eyes (postnatal mice) or heads (embryos) were fixed in Pen-Fix (Richard Allen Scientific, Kalamazoo, MI) for two hours prior to paraffin embedding. Serial 6 μm sections were cut and stained by hematoxylin and eosin using standard methods and visualized with a light microscope. The expression pattern of β- and γ-crystallins was determined by incubating deparaffinized sections with rabbit anti-bovine β-crystallin or rabbit anti-bovine γ-crystallin primary antibodies (gifts of Samuel Zigler, Johns Hopkins University, Baltimore, MD). Detection was done with an anti-rabbit Dako Envision horseradish peroxidase kit (Dako Laboratories, Carpinteria, CA).

Further histological analysis was performed by fixing lenses in 2.5% glutaraldehyde, 2% formaldehyde, and 0.1M cacodylate, pH 7.4, at room temperature for approximately 48 hours. Tissue was rinsed for 15 minutes in water, dehydrated by a series of exchanges in 50%, 70%, and 90% ethanol, and then three times in 100% ethanol, for 15 minutes each. Tissue was then immersed in three 15-minute washes with propylene oxide, followed by immersion in a 1:1 mix of propylene oxide and Embed 812 (EMS, Hatfield, PA) overnight. After four hours in 100% Embed 812, the resin was polymerized at 60°C for approximately 30 hours. Sections, 1 μm in thickness, were stained with Toluidine Blue. Images were adjusted in Photoshop, using Level control, in order to use the full extent of the input ranges.

4.4. Scanning Electron Microscopy

Scanning electron microscopy was performed on adult *Sip1* cKO and wild type lenses as previously described (Duncan et al., 2000; Firtina et al., 2009).

4.5. Immunofluorescence

Immunofluorescence was performed as previously described (Reed et al., 2001). Briefly, eyes or lenses were embedded in Tissue Freezing Media, TFM (Triangle Biomedical, Durham, NC), and 16 μm thick frozen sections were prepared, placed on Colorfrost Plus glass slides (Fisher Scientific, Pittsburgh, PA), and stored at -80°C until use. Slides were fixed in 1:1 acetone/methanol or 4% paraformaldehyde in 1xPBS and blocked in 1% BSA in 1x Phosphate Buffered Saline (PBS) for one hour. Tissue was then covered with a dilution of primary antibody for one hour at room temperature. Slides were washed three times in 1xPBS, then incubated for one hour with a 1:2000 dilution of DRAQ5 (Biostatus Limited, Leicestershire, United Kingdom) mixed with a 1:200 dilution of goat anti-rabbit IgG conjugated to Alexa Fluor 568 (Invitrogen, A11057). Slides were again washed three times in 1xPBS, sections covered with *p*-phenylenediamine antifade media (Johnson & Nogueira Araujo, 1981), and cover slipped. All experiments were repeated with at least three biological replicates and slides were viewed using either a Zeiss 510 LSM or a Zeiss 780 LSM confocal microscope. All comparisons of expression pattern were done between slides

generated from the same staining experiment and imaged on the same day under the same imaging settings. In some cases, brightness and/or contrast of obtained images was adjusted in Adobe Photoshop for optimum viewing on diverse computer screens, however, in all cases, such adjustments were applied equally to both experimental and control images to retain the validity of comparison.

Sip1 immunostaining followed a similar procedure as above, but slides were instead blocked with 5% normal goat serum with 0.3% Triton X-100 in 1x Tris Buffered Saline (TBS) for two hours, incubated in 1:100 dilution of rabbit anti-Sip1 primary antibody overnight at 4°C, and washed with 1xTBS. Other primary antibodies and respective dilutions utilized in this study can be found in Supplemental Table 1.

Epithelial whole mounts were also dissected from adult *Sip1* cKO and C57Bl/6<har> mouse lenses, mounted as previously described (White et al., 2007), and immunostained using similar techniques as described above. Whole lens staining was done using intact adult and E16.5 lenses that were fixed in 4% paraformaldehyde for one to two hours and washed in 1xPBS with 0.1% Triton X-100. The lenses were then stained with a 1:200 dilution of Alexa Fluor 568nm labeled Phalloidin and a 1:2000 dilution of DRAQ5 in 1xPBS with 0.25% Triton X-100. A final series of washes was done in 1xPBS and the lenses stored at 4°C until imaging. For meridional row imaging, lenses were oriented on their equatorial side as previously described (Bassnett and Shi, 2010) in a glass bottomed Nunc Lab-Tek chamber (Nalge Nunc International, Rochester, NY) filled with 2% agarose in 1xPBS and imaged on an inverted confocal microscope (Zeiss 5 Live DUO, Thornwood, NY). Three-dimensional data sets were collected and cortical fiber cells were cropped from the image using a 3D software program (Volocity 4, PerkinElmer Inc.) to allow for better viewing of the meridional rows. Maximum intensity projections were then used to flatten the images in two dimensions.

4.6. Western Blotting and Coomassie Staining

Adult and E16.5 lenses from *Sip1* cKO and wild type animals were harvested and homogenized in ice-cold lysis buffer (50 mM Tris-HCl, pH 8.0, 150 mM NaCl, 1% Nonidet P-40, 0.5% sodium deoxycholate, 0.1% SDS) with Halt protease and phosphatase inhibitor mixture (Thermo Scientific, Rockford, IL). The extract was centrifuged at 16,000 x g for 30 minutes to remove the insoluble material and protein levels were quantified. For Coomassie stained gels, 20 μg of total protein was separated by SDS-polyacrylamide gel electrophoresis (PAGE) and the gel was stained with SimplyBlue SafeStain (Invitrogen, Grand Island, NY) according to the manufacturer. For western blots, 40 μg of total protein was separated by SDS-PAGE and transferred to nitrocellulose membranes (Bio-Rad, Hercules, CA). The membranes were blocked with 5% BSA and 0.01% Tween 20 in 1xTBS for one hour at room temperature or overnight at 4°C with Superblock T20 blocking buffer (Thermo Scientific, Rockford, IL). Membranes were then incubated in an appropriate dilution of rabbit primary antibodies in blocking buffer (Supplemental Table 1) for two hours at room temperature or overnight at 4°C followed by incubation with a 1:20,000 dilution of horseradish peroxidase (HRP)-conjugated secondary anti-rabbit antibody (Calbiochem, San Diego, CA) for one hour at room temperature. Signals were detected using an ECL detection

kit (Amersham Biosciences, Piscataway, NY) and quantified with a FluorChem Q SA imager (ProteinSimple, San Jose, CA).

4.7. RNA-Sequencing Analysis

Lenses were collected from *Sip1* cKO and wild type lenses at E15.5 (30 lenses per biological replicate; three independent biological replicates analyzed for each genotype) using micro dissection, during which the retina, blood vessels, and cornea were carefully removed with forceps. Total RNA was extracted using the SV Total RNA Isolation System (Invitrogen). Messenger RNA was purified from the total RNA samples using Oligo dT conjugated magnetic beads, and converted to adaptor-tagged, single-end fragments which were then used for cluster generation onto a TruSeq v3 flow cell according to the Illumina® TruSeq™ RNA Sample Preparation Kit v2. Sequencing was done using the SBS Sequencing Kit on an Illumina HiSeq 2000 Sequencer (University of Delaware Genotyping and Sequencing Center) with 50-cycle single-end reads. The images were analyzed using the Illumina Pipeline software (version RTA 1.13.48 / CASAVA 1.8.2), and bases were called and translated to generate FASTQ sequence files.

Overall quality of the Illumina HiSeq datasets was assessed using FastQC (http://www.bioinformatics.babraham.ac.uk/projects/fastqc/) and CLC Genomics Workbench (CLC Bio, Aarhus, Denmark). Subsequent data processing was performed using the CLC Genomics Workbench and Genomics Server (version 5.1). Briefly, sequences were trimmed to remove common Illumina adapters and poly-A, and to remove low quality sequence ends (ambiguous base limit: 0; quality limit: 0.01). Following trimming, all sequences shorter than 35 bp were discarded. High quality sequences were aligned to the *Mus musculus* reference genome (Build NCBI-M37.65 ENSEMBL/MGI annotations) using the CLC RNA-Seq reference mapping algorithm (length parameter: 0.9, identity: 0.8). Non-specifically mapping reads were not considered in downstream statistical analysis. Reads per kilobase per million (RPKM) values were calculated to rank gene expression. Observed counts were quantile normalized (reviewed in Bolstad et al., 2003) before differential expression analysis using the beta binomial method of Baggerly *et al.* (2003) with FDR (False Discovery Rate) correction for multiple comparisons (Benjamini and Hochberg, 1995). All RNA-Seq datasets used in this study have been deposited in Gene Expression Omnibus (GEO accession GSE49949 for all data series). Only genes with mean unnormalized RPKM values greater than two for either the wild type or *Sip1* cKO were investigated, estimated to correspond to approximately one mRNA molecule per cell (based on the estimate that typical mammalian cells contain 500,000 molecules of mRNA (Bryant and Manning, 1998) although cells can vary significantly in mRNA content (Islam et al., 2011)). A minimum change in RPKM greater than two was also used in further analysis. Additionally, only genes with a *p*-value less than 0.05 (for a 95% confidence interval) and more than a 2.5 fold change in normalized RPKM value are reported. This fold change threshold was chosen based on experimental data comparing relative gene expression between E15.5 lenses from mixed background *Sip1* f/f no Cre control mice and inbred C57Bl/6<har> mice (GEO accession GSE49949) which indicated that a large proportion of changes below 2.5 fold are likely due to variation in genetic background, not the *Sip1* gene deletion. Further, expression of Klf4 and Klf5, transcription factors abundant in the corneal epithelium (Swamynathan et

al., 2007; Kenchegowda et al., 2011) were greatly below the 2 RPKM cutoff for significant expression in both wild type and mutant samples, showing that the samples lacked appreciable corneal contamination arising during the dissection. Similarly, Pecam1, a marker expressed abundantly in blood vessels of the eye (Ferrari et al., 2013), was detected at only 2-3 RPKM in all samples used in our analysis, with no significant differences between wild type and *Sip1* cKO, indicating that changes in gene expression in the Sip1 cKO lens are bona fide and are not attributable to contamination by neighboring tissues during dissection.

4.8. Ingenuity Pathway Analysis, Evaluation of Normal Gene Expression, and Promoter Binding Site Exploration

The final list of differentially expressed genes obtained from the RNA-Seq analysis was then subjected to Ingenuity Pathway Analysis (IPA; Ingenuity Systems Inc., Redwood City, CA) to identify potential co-regulated pathways.

The list of differentially regulated genes in *Sip1* mutant lenses was also compared to those differentially regulated and enriched during normal early lens development. The microarray datasets for E10.5 and E12.5 lens as well as whole embryonic tissue without eyes (whole body, WB) used for this analysis were generated previously on the Affymetrix Mouse Genome 430 2.0 Array and used as foundation data for the web-based resource *iSyTE* (Lachke et al., 2012). Genes found to be differentially regulated in the *Sip1* cKO lens by RNA-Seq were then compared against this lens microarray database and scored into the following categories: (1) significantly downregulated ($p < 0.05$) as the lens transitions from E10.5 to E12.5; (2) significantly upregulated ($p < 0.05$) as the lens transitions from E10.5 to E12.5; (3) not significantly expressed ($p > 0.05$, detection p-value) in the E10.5 and E12.5 lens as determined by Affymetrix microarrays; (4) not found in the Affymetrix dataset; and (5) expressed but levels are not significantly different between E10.5 and the E12.5 lens. When multiple probes were found to represent a single candidate gene, probes that displayed the highest expression values in any of the datasets (lens or WB) were generally selected for representing the expression pattern for the candidate gene. All original microarray datasets used in this study have already been deposited in Gene Expression Omnibus (GEO) with series accession GSE32334 as part of the *iSyTE* study.

For a subset of the genes found to be differentially expressed in the *Sip1* cKOs, the Eukaryotic Promoter Database (http://epd.vital-it.ch/) was used to obtain the -2500 to +50 promoter region relative to the known +1 transcription start site. A transcription factor binding search was then completed on these sequences using TFSearch (http://www.cbrc.jp/research/db/TFSEARCH.html) using a threshold of 85.0 (default). This analysis reported the potential binding sites for numerous transcription factors in the promoter region submitted, including the Zeb binding sites. The position in the promoter sequence was then determined and the consensus sequence was highlighted.

4.9. Quantitative Reverse Transcription – Polymerase Chain Reaction (qRT-PCR)

Three additional biological replicates for each genotype (independent samples from those used for RNA-Seq) were collected and the RNA was used to synthesize cDNA using the

RT^2qPCR Primer Assay (SABiosciences) according to the manufacturer's instructions. qRT-PCR was performed using an ABI Prism 7300 Sequence Detection System. Samples were prepared in a MicroAmp® Optical 96-Well Reaction Plate. Each well contained: 1 μL of cDNA, 12.5 μL of SYBR Green Master Mix (SABiosciences), 1 μL each of forward and reverse primers, and H_2O to 25 μL. The primer sets used for this analysis are provided in Supplemental Table 2. Mouse β2-Microglobulin (SABioscience, PPM03562A) was used as an internal control. Statistical analyses were done using log (base 10) transformed data in a nested ANOVA. The mean and standard deviation (S.D.) were then calculated for the log transformed data and subsequently back transformed, thus providing the mean fold change, a positive standard deviation, and a negative standard deviation.

Supplementary Material

Refer to Web version on PubMed Central for supplementary material.

Acknowledgments

We would like to thank Dr. Hisato Kondoh/Dr. Yujiro Higashi and Dr. Michael Robinson for providing the Sip1 flox mice and MLR10 Cre mice, respectively. Dr. Yan Wang for her support and laboratory skills. Anne Terrell and Brittany Riggio for their help with the RNA-Seq lens collection. RNA-Seq data was obtained with the help of Brewster Kingham at the University of Delaware Sequencing Center, Sean Blake at Global Biologics (Columbia, Missouri), and Dr. Shawn Polson with support from the University of Delaware Center for Bioinformatics and Computational Biology Core Facility (made possible through funding from the NIH National Center for Research Resources (5 P20 RR016472-12), the NIH National Institute of General Medical Sciences (8 P20 GM103446-12), and National Science Foundation EPSCoR (EPS-081425)). This work was funded through grant NEI grant, EY12221 supporting MD; the University of Delaware Chemistry-Biology Interface (CBI) Program supporting AM; NEI grant R01EY021505-01 supporting SL; the Vision Research Core Grant P30-EY012576 supporting PF; COBRE core grant 8P20GM103464-08 (RM) supporting the Nemours proteomics core; and 1S10 (RR027273-01) which funded the acquisition of the confocal microscope used in this study.

References

Adam MP, Schelley S, Gallagher R, Brady AN, Barr K, Blumberg B, Shieh JT, Graham J, Slavotinek A, Martin M, Keppler-Noreuil K, Storm AL, Hudgins L. Clinical features and management issues in Mowat-Wilson syndrome. Am J Med Genet A. 2006; 140:2730–2741. [PubMed: 17103451]

Ariss M, Natan K, Friedman N, Traboulsi EI. Ophthalmologic abnormalities in Mowat-Wilson syndrome and a mutation in ZEB2. Ophthalmic Genet. 2012; 33:159–160. [PubMed: 22486326]

Ashery-Padan R, Marquardt T, Zhou X, Gruss P. Pax6 activity in the lens primordium is required for lens formation and for correct placement of a single retina in the eye. Genes Dev. 2000; 14:2701–2711. [PubMed: 11069887]

Baggerly KA, Deng L, Morris JS, Aldaz CM. Differential expression in SAGE: accounting for normal between-library variation. Bioinformatics. 2003; 19:1477–1483. [PubMed: 12912827]

Bassez G, Camand OJ, Cacheux V, Kobetz A, Dastot-Le Moal F, Marchant D, Catala M, Abitbol M, Goossens M. Pleiotropic and diverse expression of ZFHX1B gene transcripts during mouse and human development supports the various clinical manifestations of the “Mowat-Wilson” syndrome. Neurobiol Dis. 2004; 15:240–250. [PubMed: 15006694]

Bassnett S. Three-dimensional reconstruction of cells in the living lens: the relationship between cell length and volume. Exp Eye Res. 2005; 81:716–723. [PubMed: 15963502]

Bassnett S, Shi Y. A method for determining cell number in the undisturbed epithelium of the mouse lens. Mol Vis. 2010; 16:2294–2300. [PubMed: 21139698]

Benjamini Y, Hochberg Y. Controlling the False Discovery Rate: A Practical and Powerful Approach to Multiple Testing. Journal of the Royal Statistical Society. Series B (Methodological). 1995; 57:289–300.

Bindels S, Mestdagt M, Vandewalle C, Jacobs N, Volders L, Noel A, van Roy F, Berx G, Foidart JM, Gilles C. Regulation of vimentin by SIP1 in human epithelial breast tumor cells. Oncogene. 2006; 25:4975–4985. [PubMed: 16568083]

Bolstad BM, Irizarry RA, Astrand M, Speed TP. A comparison of normalization methods for high density oligonucleotide array data based on variance and bias. Bioinformatics. 2003; 19:185–193. [PubMed: 12538238]

Bryant S, Manning DL. Isolation of messenger RNA. Methods Mol Biol. 1998; 86:61–64. [PubMed: 9664454]

Caneparo L, Huang YL, Staudt N, Tada M, Ahrendt R, Kazanskaya O, Niehrs C, Houart C. Dickkopf-1 regulates gastrulation movements by coordinated modulation of Wnt/beta catenin and Wnt/PCP activities, through interaction with the Dally-like homolog Knypek. Genes Dev. 2007; 21:465–480. [PubMed: 17322405]

Chauhan BK, Reed NA, Zhang W, Duncan MK, Kilimann MW, Cvekl A. Identification of genes downstream of Pax6 in the mouse lens using cDNA microarrays. J Biol Chem. 2002; 277:11539–11548. [PubMed: 11790784]

Chen Y, Stump RJ, Lovicu FJ, Shimono A, McAvoy JW. Wnt signaling is required for organization of the lens fiber cell cytoskeleton and development of lens three-dimensional architecture. Dev Biol. 2008; 324:161–176. [PubMed: 18824165]

Chua HL, Bhat-Nakshatri P, Clare SE, Morimiya A, Badve S, Nakshatri H. NF-kappaB represses E-cadherin expression and enhances epithelial to mesenchymal transition of mammary epithelial cells: potential involvement of ZEB-1 and ZEB-2. Oncogene. 2007; 26:711–724. [PubMed: 16862183]

Cvekl A, Duncan MK. Genetic and epigenetic mechanisms of gene regulation during lens development. Prog Retin Eye Res. 2007; 26:555–597. [PubMed: 17905638]

Cvekl A, Piatigorsky J. Lens development and crystallin gene expression: many roles for Pax-6. Bioessays. 1996; 18:621–630. [PubMed: 8760335]

Cvekl A, Sax CM, Li X, McDermott JB, Piatigorsky J. Pax-6 and lens-specific transcription of the chicken delta 1-crystallin gene. Proc Natl Acad Sci U S A. 1995; 92:4681–4685. [PubMed: 7753864]

Cvekl A, Yang Y, Chauhan BK, Cveklova K. Regulation of gene expression by Pax6 in ocular cells: a case of tissue-preferred expression of crystallins in lens. Int J Dev Biol. 2004; 48:829–844. [PubMed: 15558475]

Duncan MK, Cvekl A, Li X, Piatigorsky J. Truncated forms of Pax-6 disrupt lens morphology in transgenic mice. Invest Ophthalmol Vis Sci. 2000; 41:464–473. [PubMed: 10670477]

Duncan MK, Haynes JI 2nd, Cvekl A, Piatigorsky J. Dual roles for Pax-6: a transcriptional repressor of lens fiber cell-specific beta-crystallin genes. Mol Cell Biol. 1998; 18:5579–5586. [PubMed: 9710641]

Espinosa-Parrilla Y, Amiel J, Auge J, Encha-Razavi F, Munnich A, Lyonnet S, Vekemans M, Attie-Bitach T. Expression of the SMADIP1 gene during early human development. Mech Dev. 2002; 114:187–191. [PubMed: 12175509]

Ferrari G, Hajrasouliha AR, Sadrai Z, Ueno H, Chauhan SK, Dana R. Nerves and neovessels inhibit each other in the cornea. Invest Ophthalmol Vis Sci. 2013; 54:813–820. [PubMed: 23307967]

Firtina Z, Danysh BP, Bai X, Gould DB, Kobayashi T, Duncan MK. Abnormal expression of collagen IV in lens activates unfolded protein response resulting in cataract. J Biol Chem. 2009; 284:35872–35884. [PubMed: 19858219]

Galuska D, Kotova O, Barres R, Chibalina D, Benziane B, Chibalin AV. Altered expression and insulin-induced trafficking of Na+-K+-ATPase in rat skeletal muscle: effects of high-fat diet and exercise. Am J Physiol Endocrinol Metab. 2009; 297:E38–49. [PubMed: 19366873]

Garavelli L, Donadio A, Zanacca C, Banchini G, Della Giustina E, Bertani G, Albertini G, Del Rossi C, Zweier C, Rauch A, Zollino M, Neri G. Hirschsprung disease, mental retardation, characteristic facial features, and mutation in the gene ZFHX1B (SIP1): confirmation of the Mowat-Wilson syndrome. Am J Med Genet A. 2003; 116A:385–388. [PubMed: 12522797]

Garavelli L, Mainardi PC. Mowat-Wilson syndrome. Orphanet J Rare Dis. 2007; 2:42. [PubMed: 17958891]

Gautreau A, Ho HY, Li J, Steen H, Gygi SP, Kirschner MW. Purification and architecture of the ubiquitous Wave complex. Proc Natl Acad Sci U S A. 2004; 101:4379–4383. [PubMed: 15070726]

Goossens S, Janzen V, Bartunkova S, Yokomizo T, Drogat B, Crisan M, Haigh K, Seuntjens E, Umans L, Riedt T, Bogaert P, Haenebalcke L, Berx G, Dzierzak E, Huylebroeck D, Haigh JJ. The EMT regulator Zeb2/Sip1 is essential for murine embryonic hematopoietic stem/progenitor cell differentiation and mobilization. Blood. 2011; 117:5620–5630. [PubMed: 21355089]

Grabitz AL, Duncan MK. Focus on molecules: Smad Interacting Protein 1 (Sip1, ZEB2, ZFHX1B). Exp Eye Res. 2012; 101:105–106. [PubMed: 20868684]

Graw J. Eye development. Curr Top Dev Biol. 2010; 90:343–386. [PubMed: 20691855]

Grindley JC, Davidson DR, Hill RE. The role of Pax-6 in eye and nasal development. Development. 1995; 121:1433–1442. [PubMed: 7789273]

Higashi Y, Maruhashi M, Nelles L, Van de Putte T, Verschueren K, Miyoshi T, Yoshimoto A, Kondoh H, Huylebroeck D. Generation of the floxed allele of the SIP1 (Smad-interacting protein 1) gene for Cre-mediated conditional knockout in the mouse. Genesis. 2002; 32:82–84. [PubMed: 11857784]

Islam S, Kjallquist U, Moliner A, Zajac P, Fan JB, Lonnerberg P, Linnarsson S. Characterization of the single-cell transcriptional landscape by highly multiplex RNA-seq. Genome Res. 2011; 21:1160–1167. [PubMed: 21543516]

Jeub M, Emrich M, Pradier B, Taha O, Gailus-Durner V, Fuchs H, de Angelis MH, Huylebroeck D, Zimmer A, Beck H, Racz I. The transcription factor Smad-interacting protein 1 controls pain sensitivity via modulation of DRG neuron excitability. Pain. 2011; 152:2384–2398. [PubMed: 21862221]

Jimenez-Asensio J, Colvis CM, Kowalak JA, Duglas-Tabor Y, Datiles MB, Moroni M, Mura U, Rao CM, Balasubramanian D, Janjani A, Garland D. An atypical form of alphaB-crystallin is present in high concentration in some human cataractous lenses. Identification and characterization of aberrant N- and C-terminal processing. J Biol Chem. 1999; 274:32287–32294. [PubMed: 10542268]

Kenchegowda D, Swamynathan S, Gupta D, Wan H, Whitsett J, Swamynathan SK. Conditional disruption of mouse Klf5 results in defective eyelids with malformed meibomian glands, abnormal cornea and loss of conjunctival goblet cells. Dev Biol. 2011; 356:5–18. [PubMed: 21600198]

Lachke SA, Ho JW, Kryukov GV, O'Connell DJ, Aboukhalil A, Bulyk ML, Park PJ, Maas RL. iSyTE: integrated Systems Tool for Eye gene discovery. Invest Ophthalmol Vis Sci. 2012; 53:1617–1627. [PubMed: 22323457]

Lovicu FJ, McAvoy JW. Growth factor regulation of lens development. Dev Biol. 2005; 280:1–14. [PubMed: 15766743]

Maddala R, Chauhan BK, Walker C, Zheng Y, Robinson ML, Lang RA, Rao PV. Rac1 GTPase-deficient mouse lens exhibits defects in shape, suture formation, fiber cell migration and survival. Dev Biol. 2011; 360:30–43. [PubMed: 21945075]

McKinsey GL, Lindtner S, Trzcinski B, Visel A, Pennacchio LA, Huylebroeck D, Higashi Y, Rubenstein JL. Dlx1&2-dependent expression of Zfhx1b (Sip1, Zeb2) regulates the fate switch between cortical and striatal interneurons. Neuron. 2013; 77:83–98. [PubMed: 23312518]

Miquelajauregui A, Van de Putte T, Polyakov A, Nityanandam A, Boppana S, Seuntjens E, Karabinos A, Higashi Y, Huylebroeck D, Tarabykin V. Smad-interacting protein-1 (Zfhx1b) acts upstream of Wnt signaling in the mouse hippocampus and controls its formation. Proc Natl Acad Sci U S A. 2007; 104:12919–12924. [PubMed: 17644613]

Moll R, Franke WW, Schiller DL, Geiger B, Krepler R. The catalog of human cytokeratins: Patterns of expression in normal epithelia, tumors and cultured cells. Cell. 1982; 31:11–24. [PubMed: 6186379]

Mowat DR, Wilson MJ, Goossens M. Mowat-Wilson syndrome. J Med Genet. 2003; 40:305–310. [PubMed: 12746390]

Nelles L, Van de Putte T, van Grunsven L, Huylebroeck D, Verschueren K. Organization of the mouse Zfhx1b gene encoding the two-handed zinc finger repressor Smad-interacting protein-1. Genomics. 2003; 82:460–469. [PubMed: 13679026]

Nishimura G, Manabe I, Tsushima K, Fujiu K, Oishi Y, Imai Y, Maemura K, Miyagishi M, Higashi Y, Kondoh H, Nagai R. DeltaEF1 mediates TGF-beta signaling in vascular smooth muscle cell differentiation. Dev Cell. 2006; 11:93–104. [PubMed: 16824956]

Pajoohesh-Ganji A, Pal-Ghosh S, Tadvalkar G, Stepp MA. Corneal goblet cells and their niche: implications for corneal stem cell deficiency. Stem Cells. 2012; 30:2032–2043. [PubMed: 22821715]

Piatigorsky J. Lens differentiation in vertebrates. A review of cellular and molecular features. Differentiation. 1981; 19:134–153. [PubMed: 7030840]

Ponce A, Sorensen C, Takemoto L. Role of short-range protein interactions in lens opacifications. Mol Vis. 2006; 12:879–884. [PubMed: 16917488]

Pontoriero GF, Smith AN, Miller LA, Radice GL, West-Mays JA, Lang RA. Co-operative roles for E-cadherin and N-cadherin during lens vesicle separation and lens epithelial cell survival. Dev Biol. 2009; 326:403–417. [PubMed: 18996109]

Rakeman AS, Anderson KV. Axis specification and morphogenesis in the mouse embryo require Nap1, a regulator of WAVE-mediated actin branching. Development. 2006; 133:3075–3083. [PubMed: 16831833]

Reed NA, Oh DJ, Czymmek KJ, Duncan MK. An immunohistochemical method for the detection of proteins in the vertebrate lens. J Immunol Methods. 2001; 253:243–252. [PubMed: 11384685]

Remacle JE, Kraft H, Lerchner W, Wuytens G, Collart C, Verschueren K, Smith JC, Huylebroeck D. New mode of DNA binding of multi-zinc finger transcription factors: deltaEF1 family members bind with two hands to two target sites. EMBO J. 1999; 18:5073–5084. [PubMed: 10487759]

Robertson LJ, David LL, Riviere MA, Wilmarth PA, Muir MS, Morton JD. Susceptibility of ovine lens crystallins to proteolytic cleavage during formation of hereditary cataract. Invest Ophthalmol Vis Sci. 2008; 49:1016–1022. [PubMed: 18326725]

Sax CM, Farrell FX, Zehner ZE, Piatigorsky J. Regulation of vimentin gene expression in the ocular lens. Dev Biol. 1990; 139:56–64. [PubMed: 2328840]

Sekido R, Murai K, Funahashi J, Kamachi Y, Fujisawa-Sehara A, Nabeshima Y, Kondoh H. The delta-crystallin enhancer-binding protein delta EF1 is a repressor of E2-box-mediated gene activation. Mol Cell Biol. 1994; 14:5692–5700. [PubMed: 8065305]

Seuntjens E, Nityanandam A, Miquelajauregui A, Debruyn J, Stryjewska A, Goebbels S, Nave KA, Huylebroeck D, Tarabykin V. Sip1 regulates sequential fate decisions by feedback signaling from postmitotic neurons to progenitors. Nat Neurosci. 2009; 12:1373–1380. [PubMed: 19838179]

Shaham O, Smith AN, Robinson ML, Taketo MM, Lang RA, Ashery-Padan R. Pax6 is essential for lens fiber cell differentiation. Development. 2009; 136:2567–2578. [PubMed: 19570848]

Steffen A, Rottner K, Ehinger J, Innocenti M, Scita G, Wehland J, Stradal TE. Sra-1 and Nap1 link Rac to actin assembly driving lamellipodia formation. EMBO J. 2004; 23:749–759. [PubMed: 14765121]

Sugiyama Y, McAvoy JW. Analysis of PCP defects in mammalian eye lens. Methods Mol Biol. 2012; 839:147–156. [PubMed: 22218899]

Swamynathan SK, Katz JP, Kaestner KH, Ashery-Padan R, Crawford MA, Piatigorsky J. Conditional deletion of the mouse Klf4 gene results in corneal epithelial fragility, stromal edema, and loss of conjunctival goblet cells. Mol Cell Biol. 2007; 27:182–194. [PubMed: 17060454]

Ueda Y, Duncan MK, David LL. Lens proteomics: the accumulation of crystallin modifications in the mouse lens with age. Invest Ophthalmol Vis Sci. 2002; 43:205–215. [PubMed: 11773033]

Van de Putte T, Maruhashi M, Francis A, Nelles L, Kondoh H, Huylebroeck D, Higashi Y. Mice lacking ZFHX1B, the gene that codes for Smad-interacting protein-1, reveal a role for multiple neural crest cell defects in the etiology of Hirschsprung disease-mental retardation syndrome. Am J Hum Genet. 2003; 72:465–470. [PubMed: 12522767]

van Grunsven LA, Schellens A, Huylebroeck D, Verschueren K. SIP1 (Smad interacting protein 1) and deltaEF1 (delta-crystallin enhancer binding factor) are structurally similar transcriptional repressors. J Bone Joint Surg Am. 2001; 83-A(Suppl 1):S40–47. [PubMed: 11263664]

Vandewalle C, Comijn J, De Craene B, Vermassen P, Bruyneel E, Andersen H, Tulchinsky E, Van Roy F, Berx G. SIP1/ZEB2 induces EMT by repressing genes of different epithelial cell-cell junctions. Nucleic Acids Res. 2005; 33:6566–6578. [PubMed: 16314317]

Vandewalle C, Van Roy F, Berx G. The role of the ZEB family of transcription factors in development and disease. Cell Mol Life Sci. 2009; 66:773–787. [PubMed: 19011757]

Verschueren K, Remacle JE, Collart C, Kraft H, Baker BS, Tylzanowski P, Nelles L, Wuytens G, Su MT, Bodmer R, Smith JC, Huylebroeck D. SIP1, a novel zinc finger/homeodomain repressor, interacts with Smad proteins and binds to 5′-CACCT sequences in candidate target genes. J Biol Chem. 1999; 274:20489–20498. [PubMed: 10400677]

Wang WL, Li Q, Xu J, Cvekl A. Lens fiber cell differentiation and denucleation are disrupted through expression of the N-terminal nuclear receptor box of NCOA6 and result in p53-dependent and p53-independent apoptosis. Mol Biol Cell. 2010; 21:2453–2468. [PubMed: 20484573]

Weng Q, Chen Y, Wang H, Xu X, Yang B, He Q, Shou W, Higashi Y, van den Berghe V, Seuntjens E, Kernie SG, Bukshpun P, Sherr EH, Huylebroeck D, Lu QR. Dual-mode modulation of Smad signaling by Smad-interacting protein Sip1 is required for myelination in the central nervous system. Neuron. 2012; 73:713–728. [PubMed: 22365546]

White TW, Gao Y, Li L, Sellitto C, Srinivas M. Optimal lens epithelial cell proliferation is dependent on the connexin isoform providing gap junctional coupling. Invest Ophthalmol Vis Sci. 2007; 48:5630–5637. [PubMed: 18055813]

Wilmarth PA, Tanner S, Dasari S, Nagalla SR, Riviere MA, Bafna V, Pevzner PA, David LL. Age-related changes in human crystallins determined from comparative analysis of post-translational modifications in young and aged lens: does deamidation contribute to crystallin insolubility? J Proteome Res. 2006; 5:2554–2566. [PubMed: 17022627]

Wride MA. Cellular and molecular features of lens differentiation: a review of recent advances. Differentiation. 1996; 61:77–93. [PubMed: 8983174]

Xia M, Hu M, Wang J, Xu Y, Chen X, Ma Y, Su L. Identification of the role of Smad interacting protein 1 (SIP1) in glioma. J Neurooncol. 2009; 97:225–232. [PubMed: 19806322]

Xie Q, Yang Y, Huang J, Ninkovic J, Walcher T, Wolf L, Vitenzon A, Zheng D, Gotz M, Beebe DC, Zavadil J, Cvekl A. Pax6 interactions with chromatin and identification of its novel direct target genes in lens and forebrain. PLoS One. 2013; 8:e54507. [PubMed: 23342162]

Xu L, Overbeek PA, Reneker LW. Systematic analysis of E-, N- and P-cadherin expression in mouse eye development. Exp Eye Res. 2002; 74:753–760. [PubMed: 12126948]

Yoshimoto A, Saigou Y, Higashi Y, Kondoh H. Regulation of ocular lens development by Smad-interacting protein 1 involving Foxe3 activation. Development. 2005; 132:4437–4448. [PubMed: 16162653]

Zhao H, Yang T, Madakashira BP, Thiels CA, Bechtle CA, Garcia CM, Zhang H, Yu K, Ornitz DM, Beebe DC, Robinson ML. Fibroblast growth factor receptor signaling is essential for lens fiber cell differentiation. Dev Biol. 2008; 318:276–288. [PubMed: 18455718]

Zhao H, Yang Y, Rizo CM, Overbeek PA, Robinson ML. Insertion of a Pax6 consensus binding site into the alphaA-crystallin promoter acts as a lens epithelial cell enhancer in transgenic mice. Invest Ophthalmol Vis Sci. 2004; 45:1930–1939. [PubMed: 15161860]

Zweier C, Thiel CT, Dufke A, Crow YJ, Meinecke P, Suri M, Ala-Mello S, Beemer F, Bernasconi S, Bianchi P, Bier A, Devriendt K, Dimitrov B, Firth H, Gallagher RC, Garavelli L, Gillessen-Kaesbach G, Hudgins L, Kaariainen H, Karstens S, Krantz I, Mannhardt A, Medne L, Mucke J, Kibaek M, Krogh LN, Peippo M, Rittinger O, Schulz S, Schelley SL, Temple IK, Dennis NR, Van der Knaap MS, Wheeler P, Yerushalmi B, Zenker M, Seidel H, Lachmeijer A, Prescott T, Kraus C, Lowry RB, Rauch A. Clinical and mutational spectrum of Mowat-Wilson syndrome. Eur J Med Genet. 2005; 48:97–111. [PubMed: 16053902]

Highlights

- Sip1 deletion before and after lens vesicle closure results in different defects
- Sip1 deletion after closure causes defects in fiber cell tip migration at E16.5
- In the adult, loss of Sip1 after lens vesicle closure causes cataract formation
- RNA-Seq identified 190 differentially expressed genes in E15.5 Sip1 knockout lenses
- Sip1 likely represses ectodermal gene expression in the lens after vesicle closure

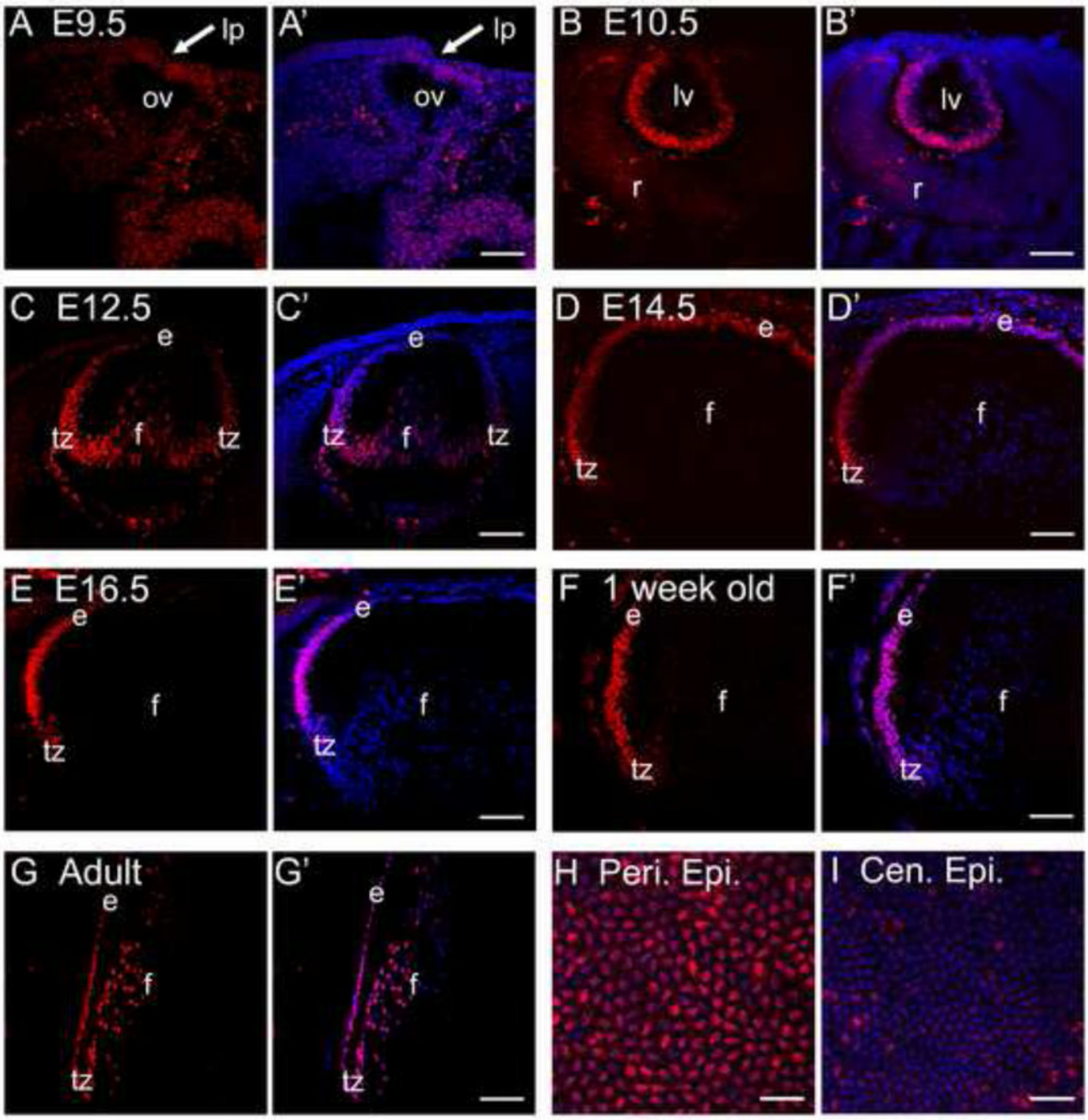

Fig. 1.

Sip1 protein expression during lens development. Very little Sip1 protein expression is observed in the wild type lens placode region (arrow) at E9.5 (A), but it is present in high levels in the cells of the posterior lens vesicle at E10.5 (B). (C) Sip1 expression is maintained in the transition zone at E12.5, but levels begin to decrease in the interior-most fiber cells. At E14.5 (D), Sip1 is expressed in the entire epithelium becoming more specific to the peripheral epithelium by E16.5 (E). Expression in the peripheral epithelium continues post-natally (F). In the adult, expression is also found in the very young cortical fiber cells

(G). Similar to the postnatal stages, adult epithelial whole mounts show Sip1 protein in the peripheral epithelium (H) with very little found in the central epithelium (I). Abbreviations: lp, lens placode; ov, optic vesicle; lv, lens vesicle; r, early retina; e, lens epithelium; f, lens fiber cells; tz, lens transition zone; peri. epi., peripheral lens epithelium; cen. epi., central lens epithelium. Prime panels (e.g. A′) show Sip1 expression (Red) merged with nuclei (DRAQ5, Blue). Scale bar = 77μm (A – G); 38μm (H, I).

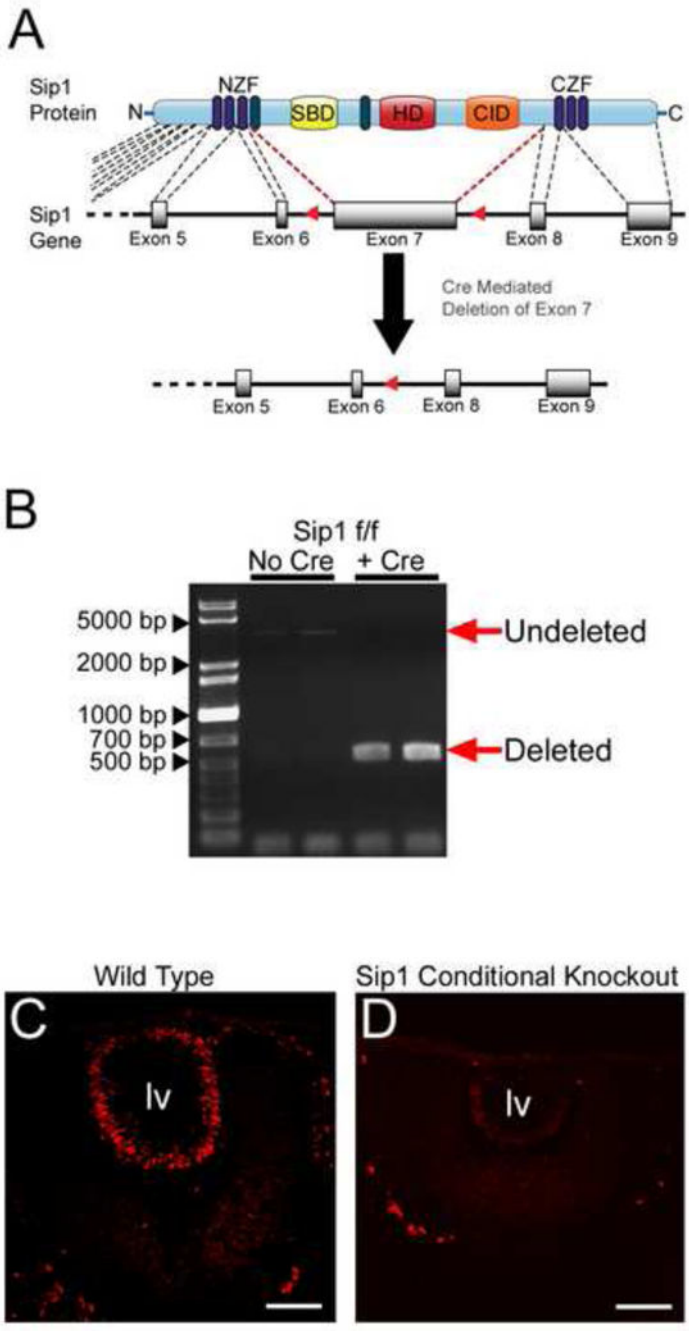

Fig. 2.

Deletion of *Sip1* from the lens. Deletion scheme (A) showing how mice harboring loxP/flox sites flanking exon 7 of *Sip1* (Higashi et al., 2002) were mated to *MLR10Cre* mice to delete the majority of the *Sip1* coding sequence. (B) Adult lens DNA was analyzed to show the loss of exon 7 (undeleted band at ∼3,268bp, deleted band at ∼542bp) in mice homozygous for the floxed allele and carrying the *MLR10 Cre* transgene. (C) Wild type Sip1 protein expression (Red) is lost in the *Sip1* cKO (D) at E10.5. Abbreviations: lv, lens vesicle. Scale Bar = 77μm.

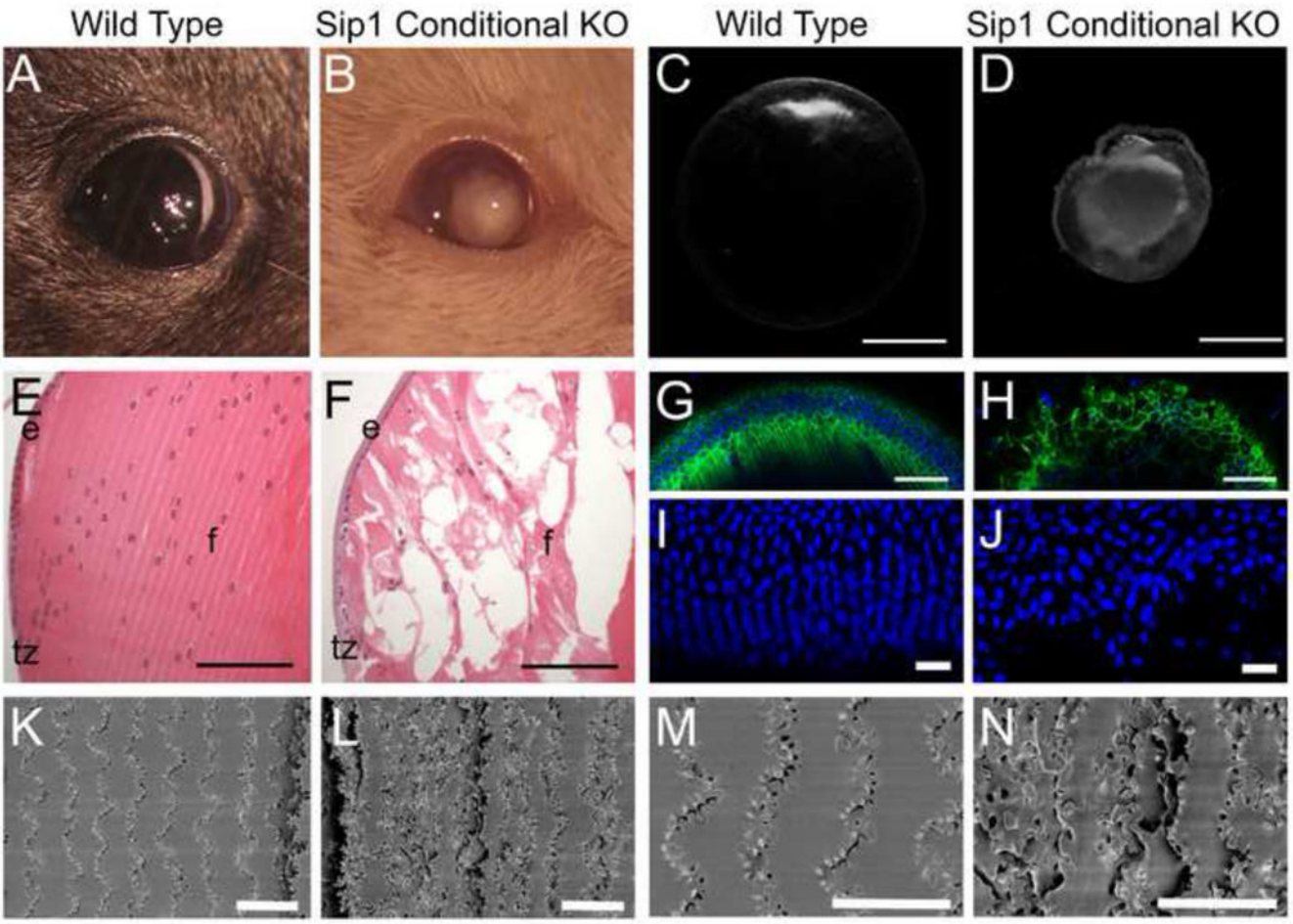

Fig. 3.

Loss of *Sip1* results in profound defects in the size, opacity, and fiber cell structure of the adult lens. Wild type (A) and *Sip1* cKO (B) mice showing obvious cataracts in the *Sip1* cKO lens. Darkfield microscopy of dissected lenses shows that *Sip1* cKO lenses (D) are altered in size and shape compared to normal lenses (C). Normal fiber cell morphology, shown by H&E stained sections (E) and whole lens F-actin staining (G), is disordered when Sip1 is lost (F, H) (Cytoplasm – Pink, Nuclei – Purple; F-Actin/Phalloidin – Green, Nuclei/DRAQ5 – Blue,). Organized meridional rows in the wild type (I) are disrupted when Sip1 is lost (J) (Nuclei/DRAQ5 – Blue). Protrusions, found along the vertices in the cortical fiber cells of the wild type lens (K, M) are disorganized in the *Sip1* cKOs (L, N). Abbreviations: e, lens epithelium; f, lens fiber cells; tz, lens transition zone. Scale Bars = 1mm (C, D); 100μm (E, F); 77μm (G, H); 22μm (I, J); 20μm (K, L); 10μm (M, N).

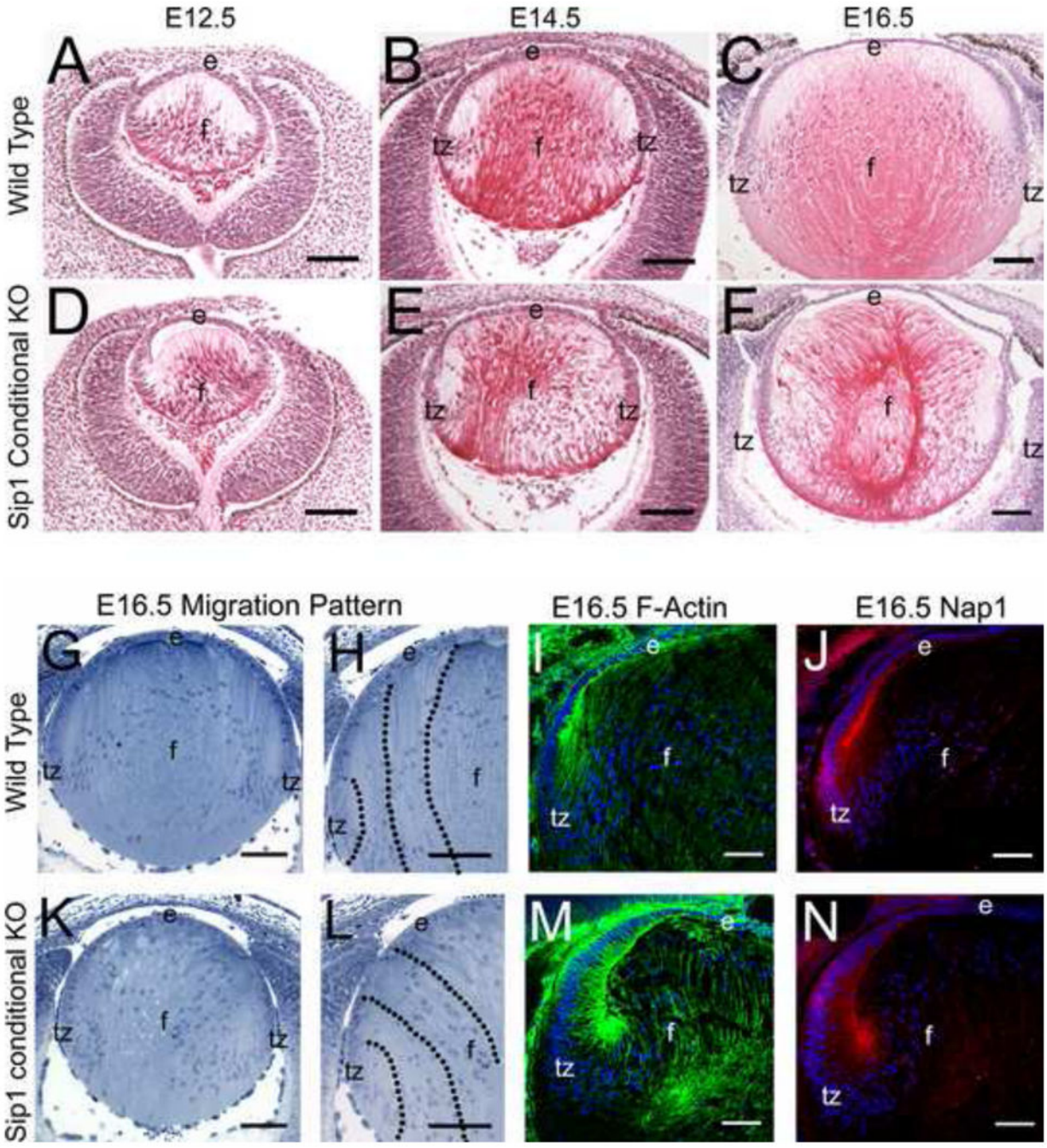

Fig. 4.

Loss *of Sip1* causes morphological abnormalities between E14.5 and 16.5. Compared to wild type lenses at E12.5 (A) and E14.5 (B), *Sip1* cKO lenses appear normal (D, E), but by E16.5 (C) the fiber cells become disorganized when *Sip1* is lost (F) (Cytoplasm – Pink, Nuclei – Purple). Toluidine-blue staining of normal E16.5 lenses (G, H) and *Sip1* cKO lenses (K, L) further highlights the disorganized morphology of the *Sip1* cKOs. Expression of F-actin (I) and the migration protein Nap1 (J), are unchanged in the knockout, although they may be mislocalized (M, N) (Nap1 – Red , F-Actin/Phalloidin – Green, Nuclei/DRAQ5 – Blue).

Abbreviations: e, lens epithelium; f, lens fiber cells; tz, lens transition zone. Scale Bars = 100μm (A – H, K, L); 74μm (I, J, M, N).

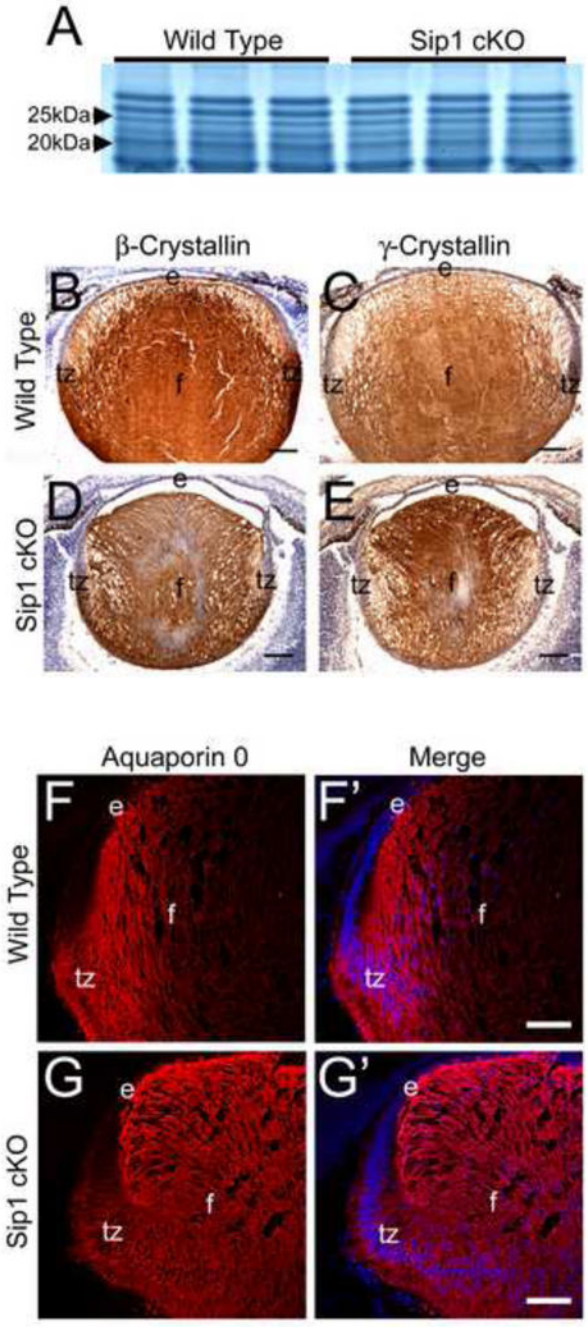

Fig. 5.

Analysis of fiber cell marker expression in *Sip1* cKO lenses shows little to no change in embryonic crystallin expression. SDS-PAGE analysis shows little to no difference in global crystallin expression at E16.5 (A). Expression of β-crystallins (B) and γ-crystallins (C) in E16.5 sections, also appears normal in the *Sip1* cKOs (D and E). Lastly, expression of Aquaporin 0, staining the fiber cell membrane in the wild type (F), also shows little difference in the *Sip1* cKOs (G), although the staining is different reflecting the observed fiber cell tip migration defect (Prime panels (e.g. F′) shows Aquaporin 0 expression (Red)

merged with nuclei (DRAQ5, Blue)). Abbreviations: e, lens epithelium; f, lens fiber cells; tz, lens transition zone. Scale Bars = 100μm (B – E); 77μm (F, G).

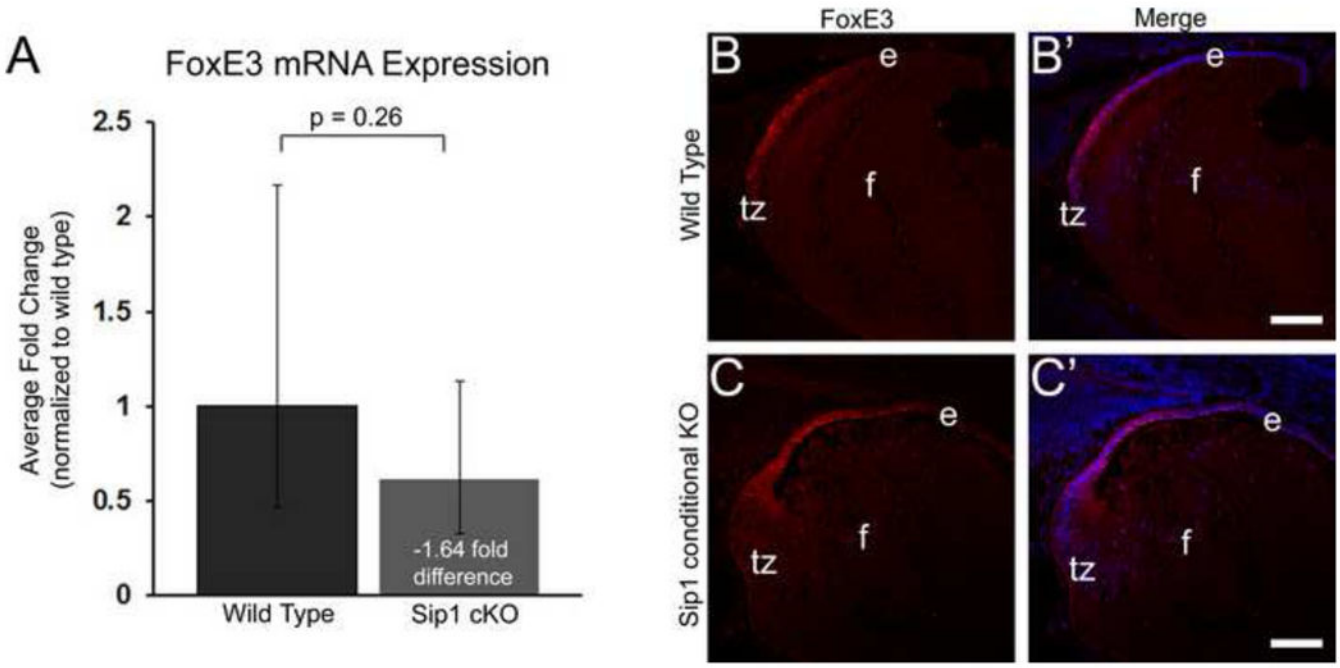

Fig. 6.

FoxE3 expression is not significantly altered in the *Sip1* cKOs at E16.5 at the RNA level (A) and the expression of FoxE3 protein in the epithelium (B) is similar in the *Sip1* knockout lens (C). Abbreviations: e, lens epithelium; f, lens fiber cells; tz, lens transition zone. Prime panels (e.g. B′) show FoxE3 expression (Red) merged with nuclei (DRAQ5, Blue), Scale Bars = 74μm.

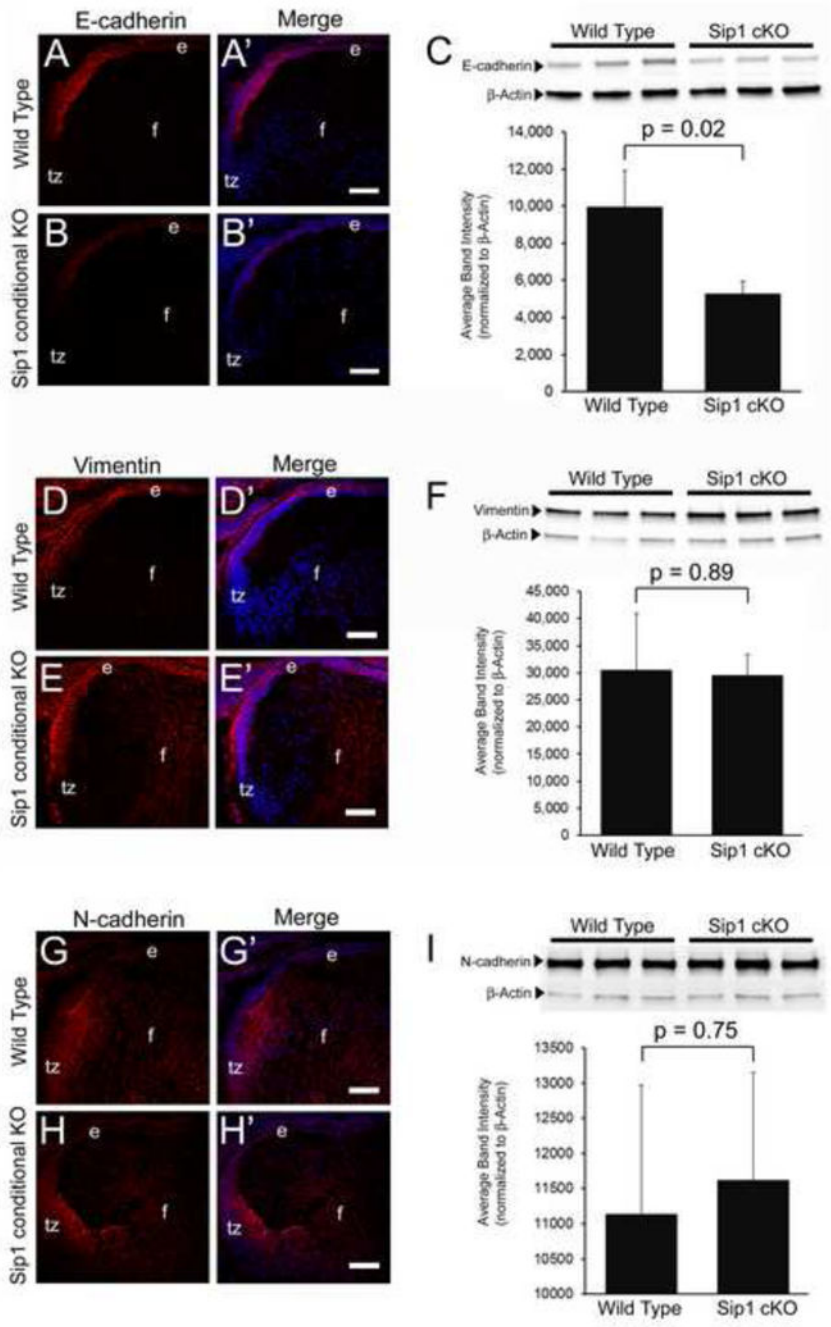

Fig. 7.

Immunofluorescence and western blot analysis of epithelial – to – mesenchymal transition (EMT) related genes, E-cadherin, Vimentin, and N-cadherin at E16.5 are contrary to cancer reserarch. E-cadherin is expressed in the lens epithelium (A) and is downregulated significantly in the *Sip1* cKOs (B) (C: $p = 0.02$) (E-cadherin – Red). However, expression is recovered in the adult (Data Not Shown). Neither Vimentin, expressed in the epithelium and fiber cells (D) (Vimentin – Red), nor N-cadherin, expressed in the fiber cells (G) (N-cadherin – Red) are significantly altered in the *Sip1* cKO (E, $p = 0.89$ and H, $p = 0.75$,

respectively). Abbreviations: e, lens epithelium; f, lens fiber cells; tz, lens transition zone. Prime panels (e.g. B′) show gene expression (Red) merged with nuclei (DRAQ5, Blue). Scale Bars = 70μm.

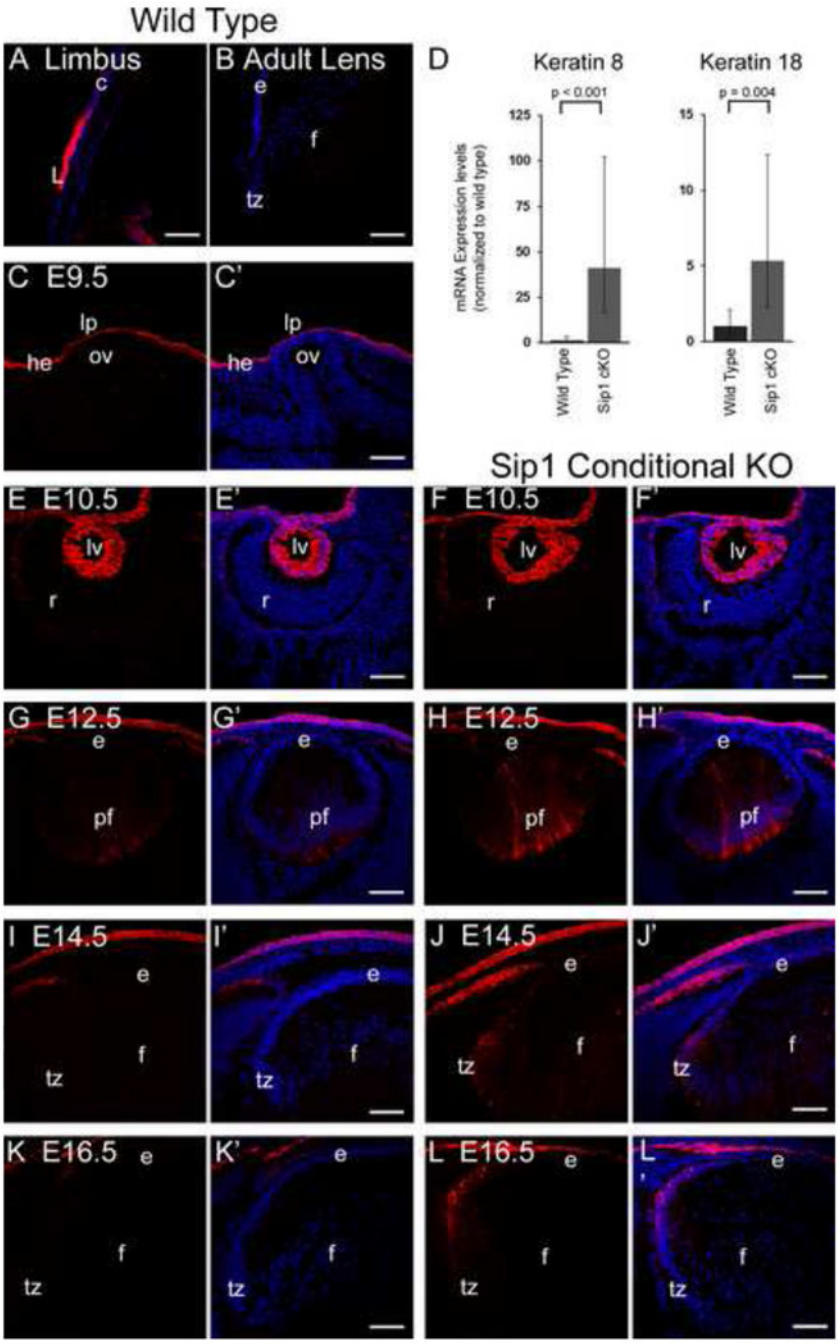

Fig. 8.

Keratin 8 is normally downregulated in the lens after fiber cell differentiation, but is retained in the *Sip1* cKOs. Prior studies show Keratin 8 is highly expressed in the limbus, confirmed here (A). Keratin 8 is absent from the adult lens (B); but is expressed in the embryonic head ectoderm at E9.5 (C). At the mRNA level (D), Keratin 8 is significantly increased 41 fold (+61/-25; *p*-value = 0.00004), while Keratin 18 is increased 5 fold (+7/-3; *p*-value = 0.004). In both the wild type (E) and *Sip1* cKO (F), Keratin 8 protein continues to be expressed at E10.5. Expression of Keratin 8 in the wild type is decreased by E12.5 (G) and undetected by

E14.5 (I) and E16.5 (K), but expression persists in the peripheral epithelium/transition zone of the *Sip1* cKOs at these stages (H, J, L). Abbreviations: ce, corneal epithelium; L, limbus; he, head ectoderm; lp, lens placode; ov, optic vesicle; lv, lens vesicle; r, early retina; e, lens epithelium; pf, posterior fiber cells; f, lens fiber cells; tz, lens transition zone. Prime panels (e.g. A′) show Keratin 8 expression (Red) merged with nuclei (DRAQ5, Blue). Scale bar = 61μm.

Table 1

RNA-Seq analysis identified 190 differentially expressed genes in the *Sip1* cKO at E15.5. A value greater than two was used as a cutoff for the un-normalized wild type reads per kilobase per million (RPKM) and *Sip1* cKO RPKM means as well as the difference between these means. After normalization, the fold change was calculated and reported here in addition to the p-value (cutoff $p < 0.05$) and false discovery rate (FDR) *p*-value correction. The final column (column 8) identifies the expression pattern of each gene during normal development from E10.5 to E12.5 as one of the following groups: significantly downregulated ($p < 0.05$) in the E10.5 lens compared to the E12.5 lens; significantly upregulated ($p < 0.05$) in the E10.5 lens compared to the E12.5 lens; not significantly expressed ($p > 0.05$, detection *p*-value) in the E10.5 and E12.5 lens as determined by Affymetrix microarrays; not found in the Affymetrix dataset; and expressed but levels are not significantly different between E10.5 and the E12.5 lens.

Gene ID	Gene Name	Fold Change	p-value	FDR p-value correction	WT RPKM means	Sip1cKO RPKM means	Normal expression change E10.5 to E12.5
Prr15	proline rich 15	**?**	1.75E-05	1.56E-04	0.02	2.22	**not significantly expressed**
Ucma	upper zone of growth plate and cartilage matrix associated	**182.3**	0	0	0.06	14.93	**not significantly expressed**
Adamts15	a disintegrin-like and metallopeptidase (reprolysin type) with thrombospondin type 1 motif, 15	**125.3**	0	0	0.02	2.24	**downregulated**
Mt1	metallothionein 1	**81.6**	0	0	0.92	87.15	**downregulated**
Aass	aminoadipate-semialdehyde synthase	**76.6**	0	0	0.14	11.85	**downregulated**
Cxcl14	chemokine (C-X-C motif) ligand 14	**58.1**	0	0	0.08	5.08	**downregulated**
Sstr1	somatostatin receptor 1	**50.0**	0	0	0.08	4.67	**not significantly expressed**
Krt8	keratin 8	**48.1**	0	0	0.07	5. 3 3	**downregulated**
Pde6b	phosphodiesterase 6B, cGMP, rod receptor, beta polypeptide	**42.5**	0	0	0.28	13.90	**not significantly expressed**
Sntg2	syntrophin, gamma 2	**40.5**	0	0	0.08	3.64	**not significantly expressed**
Igfbp2	insulin-like growth factor binding protein 2	**37.8**	1.58E-09	2.40E-08	0.70	30.86	**downregulated**
Tnnt1	troponin T1, skeletal, slow	**37.3**	0	0	0.23	10.12	**downregulated**
Aldh1a3	aldehyde dehydrogenase family 1, subfamily A3	**34.7**	0	0	0.16	6.38	**downregulated**
Dlk1	delta-like 1 homolog (Drosophila)	**33.0**	8.06E-11	1.41E-09	0.27	10.67	**downregulated**
Atp7b	ATPase, Cu++ transporting, beta polypeptide	**28.5**	0	0	0.10	3.18	**upregulated**
Igfbpl1	insulin-like growth factor binding protein-like 1	**25.3**	0	0	0.97	28.98	**not significantly expressed**

Gene ID	Gene Name	Fold Change	p-value	FDR p-value correction	WT RPKM means	Sip1cKO RPKM means	Normal expression change E10.5 to E12.5
Plxna2	plexin A2	**23.2**	0	0	0.38	10.13	**downregulated**
Best3	bestrophin 3	**20.9**	0	0	0.10	2.27	**not found**
Nlgn1	neuroligin 1	**16.2**	0	0	0.11	2.14	**unchanged**
Lgsn	lengsin, lens protein with glutamine synthetase domain	**14.4**	0	0	0.06	3.63	**not found**
Enc1	ectodermal-neural cortex 1	**14.3**	0	0	0.81	13.73	**downregulated**
Ces1e	carboxylesterase 1E	**14.1**	0	0	0.65	10.98	**not significantly expressed**
Uchl1	ubiquitin carboxy-terminal hydrolase L1	**14.0**	0	0	147.49	2086.29	**upregulated**
Rgs4	regulator of G-protein signaling 4	**11.5**	0	0	0.62	8.67	**not significantly expressed**
Entpd3	ectonucleoside triphosphate diphosphohydrolase 3	**11.2**	0	0	0.40	5.47	**unchanged**
Dkk1	dickkopf homolog 1 (Xenopus laevis)	**10.3**	0	0	0.25	2.95	**downregulated**
Myh7b	myosin, heavy chain 7B, cardiac muscle, beta	**10.0**	0	0	5.11	58.64	**not significantly expressed**
Crygs	crystallin, gamma S	**9.1**	0	0	416.21	3724.74	**upregulated**
Acss2	acyl-CoA synthetase short-chain family member 2	**9.0**	0	0	0.55	6.73	**downregulated**
Chrna4	cholinergic receptor, nicotinic, alpha polypeptide 4	**8.8**	0	0	1.84	19.15	**unchanged**
Ptprcap	protein tyrosine phosphatase, receptor type, C polypeptide-associated protein	**8.6**	0	0	0.24	2.46	**not significantly expressed**
Ptprt	protein tyrosine phosphatase, receptor type, T	**7.6**	0	0	0.41	3.80	**downregulated**
Krt18	keratin 18	**7.5**	0	0	0.58	5.27	**downregulated**
Trim55	tripartite motif-containing 55	**7.5**	0	0	0.55	4.92	**not found**
Epn3	epsin 3	**7.2**	0	0	1.98	17.30	**not significantly expressed**
Rbm20	RNA binding motif protein 20	**7.2**	0	0	0.28	2.45	**downregulated**
Fam46b	family with sequence similarity 46, member B	**7.0**	0	0	1.55	13.59	**not significantly expressed**
Podn	podocan	**6.6**	0	0	1.55	12.35	**upregulated**
Slc38a5	solute carrier family 38, member 5	**6.0**	0	0	1.36	9.91	**upregulated**
Rgmb	RGM domain family, member B	**5.8**	0	0	1.37	9.69	**downregulated**

Gene ID	Gene Name	Fold Change	p-value	FDR p-value correction	WT RPKM means	Sip1cKO RPKM means	Normal expression change E10.5 to E12.5
Dsp	desmoplakin	**5.6**	0	0	0.38	2.60	**downregulated**
Grtp1	GH regulated TBC protein 1	**5.4**	0	0	2.07	13.07	**unchanged**
Wnk2	WNK lysine deficient protein kinase 2	**5.2**	0	0	2.41	14.49	**upregulated**
Gcg	glucagon	**4.9**	0	0	26.45	152.93	**upregulated**
Rnase4	ribonuclease, RNase A family 4	**4.8**	0	0	0.47	2.57	**downregulated**
Fras1	Fraser syndrome 1 homolog (human)	**4.7**	0	0	0.52	2.93	**downregulated**
Hddc3	HD domain containing 3	**4.7**	0	0	2.45	13.90	**downregulated**
Lbh	limb-bud and heart	**4.6**	0	0	3.78	20.85	**downregulated**
Lrrc16a	leucine rich repeat containing 16A	**4.5**	0	0	1.16	6.34	**downregulated**
Gsta4	glutathione S-transferase, alpha 4	**4.5**	0	0	3.39	18.47	**downregulated**
Myb	myeloblastosis oncogene	**4.4**	0	0	2.73	15.30	**downregulated**
Tdrd9	tudor domain containing 9	**4.2**	0	0	1.31	6.82	**not significantly expressed**
Ppp2r2b	protein phosphatase 2 (formerly 2A), regulatory subunit B (PR 52), beta isoform	**4.1**	0	0	1.20	6.02	**unchanged**
Plekha7	pleckstrin homology domain containing, family A member 7	**3.8**	0	0	0.67	3.09	**downregulated**
Cyr61	cysteine rich protein 61	**3.8**	2.50E-10	4.14E-09	0.58	2.61	**downregulated**
Edaradd	EDAR (ectodysplasin-A receptor)-associated death domain	**3.8**	0	0	0.93	4.28	**downregulated**
Rapgef5	Rap guanine nucleotide exchange factor (GEF) 5	**3.8**	0	0	1.99	9.12	**upregulated**
Ckb	creatine kinase, brain	**3.8**	0	0	85.35	357.31	**upregulated**
Fbxo10	F-box protein 10	**3.7**	0	0	2.57	11.84	**unchanged**
Gmpr	guanosine monophosphate reductase	**3.7**	0	0	4.30	19.56	**unchanged**
Slc8a1	solute carrier family 8 (sodium/calcium exchanger), member 1	**3.7**	0	0	1.44	6.45	**not significantly expressed**
Asap2	ArfGAP with SH3 domain, ankyrin repeat and PH domain 2	**3.6**	0	0	2.42	11.50	**unchanged**
Cited4	Cbp/p300-interacting transactivator, with Glu/Asp-rich carboxy-terminal domain, 4	**3.6**	0	0	3.84	16.94	**unchanged**
Sh3bp4	SH3-domain binding protein 4	**3.5**	0	0	0.97	4.15	**downregulated**
R3hdml	R3H domain containing-like	**3.5**	0	0	52.37	185.59	**not found**

Gene ID	Gene Name	Fold Change	p-value	FDR p-value correction	WT RPKM means	Sip1cKO RPKM means	Normal expression change E10.5 to E12.5
Whrn	whirlin	**3.4**	0	0	2.00	8.32	**unchanged**
Adcy9	adenylate cyclase 9	**3.4**	0	0	1.39	5.76	**not significantly expressed**
Sox3	SRY-box containing gene 3	**3.3**	0	0	0.67	2.72	**unchanged**
Lingo3	leucine rich repeat and Ig domain containing 3	**3.3**	0	0	3.21	12.69	**upregulated**
Fam132a	family with sequence similarity 132, member A	**3.2**	0	0	7.96	31.16	**unchanged**
Cbl	Casitas B-lineage lymphoma	**3.2**	1.13E-13	2.60E-12	1.12	4.35	**unchanged**
Mypn	myopalladin	**3.1**	0	0	2.72	10.33	**not significantly expressed**
Prkg1	protein kinase, cGMP-dependent, type I	**3.1**	0	0	3.14	11.98	**upregulated**
Pgpep1	pyroglutamyl-peptidase I	**3.1**	0	0	11.03	40.67	**unchanged**
Cbx6	chromobox homolog 6	**3.1**	0.039	0.176	1.26	3.34	**unchanged**
Rab6b	RAB6B, member RAS oncogene family	**3.1**	0	0	2.12	7.93	**not significantly expressed**
Apln	apelin	**3.1**	0	0	0.93	3.52	**upregulated**
Mpp7	membrane protein, palmitoylated 7 (MAGUK p55 subfamily member 7)	**3.0**	0	0	1.40	4.95	**downregulated**
Gpd2	glycerol phosphate dehydrogenase 2, mitochondrial	**3.0**	0	0	1.31	4.83	**unchanged**
Zfp111	zinc finger protein 111	**3.0**	0	0	0.82	3.04	**not significantly expressed**
Iqgap1	IQ motif containing GTPase activating protein 1	**3.0**	0	0	6.14	20.86	**downregulated**
Zbtb4	zinc finger and BTB domain containing 4	**2.9**	0	0	1.47	5.15	**upregulated**
Dapl1	death associated protein-like 1	**2.9**	1.97E-05	1.74E-04	2.91	10.10	**unchanged**
Spna1	spectrin alpha 1	**2.8**	0	0	1.44	4.85	**unchanged**
Itgb8	integrin beta 8	**2.8**	0	0	0.87	2.95	**upregulated**
Rassf4	Ras association (RalGDS/AF-6) domain family member 4	**2.8**	0	0	1.17	3.97	**upregulated**
Vill	villin-like	**2.8**	0	0	1.26	4.28	**unchanged**
Polr2b	polymerase (RNA) II (DNA directed) polypeptide B	**2.8**	1.67E-06	1.74E-05	14.31	27.86	**downregulated**
Igkc	immunoglobulin kappa constant	**2.7**	2.04E-11	3.83E-10	2.39	7.82	**unchanged**

Gene ID	Gene Name	Fold Change	p-value	FDR p-value correction	WT RPKM means	Sip1cKO RPKM means	Normal expression change E10.5 to E12.5
Btg2	B-cell translocation gene 2, anti-proliferative	**2.7**	0	0	6.80	22.34	**upregulated**
Dsc2	desmocollin 2	**2.7**	8.85E-13	1.89E-11	1.39	4.61	**downregulated**
Stac2	SH3 and cysteine rich domain 2	**2.7**	0	0	6.38	20.70	**upregulated**
Jhdm1d	jumonji C domain-containing histone demethylase 1 homolog D (S. cerevisiae)	**2.7**	0	0	1.83	4.12	**unchanged**
Magi2	membrane associated guanylate kinase, WW and PDZ domain containing 2	**2.7**	0	0	3.65	9.31	**upregulated**
Cmtm7	CKLF-like MARVEL transmembrane domain containing 7	**2.6**	0	0	7.06	23.48	**unchanged**
Neo1	neogenin	**2.6**	0	0	9.54	28.47	**unchanged**
Snx29	sorting nexin 29	**2.6**	0	0	1.14	3.55	**not significantly expressed**
Hes6	hairy and enhancer of split 6 (Drosophila)	**2.6**	0	0	7.35	22.93	**unchanged**
Cyp26a1	cytochrome P450, family 26, subfamily a, polypeptide 1	**2.5**	0	0	1.70	5.32	**downregulated**
Dusp6	dual specificity phosphatase 6	**2.5**	0	0	6.56	20.05	**downregulated**
Tek	endothelial-specific receptor tyrosine kinase	**2.5**	0	0	2.71	8.31	**upregulated**
Plxna1	plexin A1	**2.5**	0	0	7.15	14.15	**upregulated**
Ehd4	EH-domain containing 4	**2.5**	0	0	1.17	3.62	**upregulated**
Cyba	cytochrome b-245, alpha polypeptide	**-2.5**	1.30E-06	1.37E-05	11.12	5.28	**upregulated**
mt-Nd6	mitochondrially encoded NADH dehydrogenase 6	**-2.5**	3.27E-11	6.00E-10	1029.84	462.16	**not significantly expressed**
Ndufa1	NADH dehydrogenase (ubiquinone) 1 alpha subcomplex, 1	**-2.5**	6.77E-09	9.58E-08	1097.02	466.07	**upregulated**
Adc	arginine decarboxylase	**-2.5**	8.40E-82	4.22E-80	11.77	5.69	**unchanged**
Gstp2	glutathione S-transferase, pi 2	**-2.6**	2.06E-15	5.42E-14	46.96	21.19	**upregulated**
Lctl	lactase-like	**-2.6**	1.35E-13	3.10E-12	31.91	14.24	**not significantly expressed**
Cxx1b	CAAX box 1 homolog B (human)	**-2.6**	4.94E-26	1.78E-24	36.85	27.53	**not significantly expressed**
Hnrnpa1	heterogeneous nuclear ribonucleoprotein A1	**-2.6**	2.92E-06	2.95E-05	268.59	212.23	**not significantly expressed**
Cnih2	cornichon homolog 2 (Drosophila)	**-2.6**	1.21E-15	3.24E-14	23.26	11.02	**upregulated**

Gene ID	Gene Name	Fold Change	p-value	FDR p-value correction	WT RPKM means	Sip1cKO RPKM means	Normal expression change E10.5 to E12.5
Pacsin3	protein kinase C and casein kinase substrate in neurons 3	**-2.6**	8.77E-38	3.65E-36	7.90	3.70	**unchanged**
Apoo	apolipoprotein O	**-2.6**	2.37E-40	1.01E-38	17.41	12.01	**unchanged**
Tppp3	tubulin polymerization-promoting protein family member 3	**-2.6**	5.90E-46	2.61E-44	33.60	15.59	**upregulated**
Hmgn3	high mobility group nucleosomal binding domain 3	**-2.7**	6.35E-19	1.97E-17	170.95	71.81	**upregulated**
Malat1	metastasis associated lung adenocarcinoma transcript 1 (non-coding RNA)	**-2.7**	4.80E-16	1.32E-14	766.15	318.63	**upregulated**
Zbtb7b	zinc finger and BTB domain containing 7B	**-2.7**	3.88E-26	1.40E-24	35.70	15.71	**not significantly expressed**
Tecrl	trans-2,3-enoyl-CoA reductase-like	**-2.7**	4.85E-52	2.25E-50	3.97	1.83	**upregulated**
Fgfbp3	fibroblast growth factor binding protein 3	**-2.7**	1.10E-56	5.19E-55	9.15	4.24	**upregulated**
Ggct	gamma-glutamyl cyclotransferase	**-2.7**	2.30E-22	7.82E-21	25.12	10.99	**upregulated**
Rpl36a	ribosomal protein L36A	**-2.7**	1.65E-16	4.72E-15	172.70	111.20	**unchanged**
Ceacam10	carcinoembryonic antigen-related cell adhesion molecule 10	**-2.7**	2.06E-11	3.87E-10	15.39	7.22	**not significantly expressed**
Cabp5	calcium binding protein 5	**-2.7**	1.53E-27	5.66E-26	4.78	2.17	**not significantly expressed**
Pgap2	post-GPI attachment to proteins 2	**-2.7**	1.32E-71	6.50E-70	25.79	11.09	**not found**
Pmp22	peripheral myelin protein 22	**-2.7**	1.26E-68	6.20E-67	103.46	43.53	**upregulated**
Prdm16	PR domain containing 16	**-2.8**	4.67E-21	1.55E-19	8.79	3.75	**unchanged**
Ceacam2	carcinoembryonic antigen-related cell adhesion molecule 2	**-2.8**	3.59E-23	1.24E-21	7.90	3.47	**not significantly expressed**
Rnf113a1	ring finger protein 113A1	**-2.8**	2.46E-28	9.22E-27	141.42	58.35	**upregulated**
S100a11	S100 calcium binding protein A11 (calgizzarin)	**-2.9**	8.35E-14	1.95E-12	57.95	22.94	**upregulated**
Ube2v1	ubiquitin-conjugating enzyme E2 variant 1	**-2.9**	4.30E-10	6.91E-09	43.07	30.23	**upregulated**
Rnaset2a	ribonuclease T2A	**-2.9**	8.01E-56	3.77E-54	122.90	94.01	**upregulated**
Ngfr	nerve growth factor receptor (TNFR superfamily, member 16)	**-3.0**	1.28E-07	1.55E-06	9.53	3.98	**upregulated**
Rpl17	ribosomal protein L17	**-3.0**	7.37E-06	6.97E-05	338.70	174.44	**upregulated**
Nat8l	N-acetyltransferase 8-like	**-3.0**	3.68E-184	1.97E-182	4.21	1.74	**not found**
Tubb2b	tubulin, beta 2B class IIB	**-3.0**	4.25E-82	2.14E-80	48.31	19.53	**upregulated**

Gene ID	Gene Name	Fold Change	p-value	FDR p-value correction	WT RPKM means	Sip1cKO RPKM means	Normal expression change E10.5 to E12.5
Gstm1	glutathione S-transferase, mu 1	**-3.1**	5.95E-76	2.96E-74	95.78	39.19	**upregulated**
Tpm2	tropomyosin 2, beta	**-3.1**	4.98E-24	1.74E-22	20.20	7.88	**upregulated**
Rpl28	ribosomal protein L28	**-3.1**	2.96E-40	1.26E-38	445.60	227.01	**unchanged**
Gpx8	glutathione peroxidase 8 (putative)	**-3.2**	6.70E-09	9.49E-08	20.35	8.93	**unchanged**
Rpl37a	ribosomal protein L37a	**-3.2**	6.43E-20	2.06E-18	472.52	328.77	**downregulated**
Fxyd1	FXYD domain-containing ion transport regulator 1	**-3.2**	2.91E-11	5.36E-10	12.09	4.67	**upregulated**
Cyp7b1	cytochrome P450, family 7, subfamily b, polypeptide 1	**-3.3**	2.50E-66	1.21E-64	3.96	1.47	**upregulated**
Tubb4	tubulin, beta 4	**-3.4**	4.18E-21	1.39E-19	17.32	6. 3 9	**upregulated**
Ccdc23	coiled-coil domain containing 23	**-3.4**	1.53E-23	5.32E-22	76.36	27.30	**upregulated**
Pla2g7	phospholipase A2, group VII (platelet-activating factor acetylhydrolase, plasma)	**-3.4**	0	0	219.38	73.90	**upregulated**
Cyb5r2	cytochrome b5 reductase 2	**-3.4**	5.52E-79	2.76E-77	3.79	1.38	**not significantly expressed**
Tubb2a	tubulin, beta 2A class IIA	**-3.4**	5.69E-46	2.52E-44	95.51	39.86	**upregulated**
Krt40	keratin 40	**-3.4**	4.00E-28	1.49E-26	3.37	1.21	**not found**
Wdr41	WD repeat domain 41	**-3.4**	1.27E-247	6.85E-246	14.38	5.00	**upregulated**
Elovl4	elongation of very long chain fatty acids (FEN1/Elo2, SUR4/Elo3, yeast)-like 4	**-3.5**	2.07E-88	1.06E-86	4.01	1.40	**upregulated**
Cpt1a	carnitine palmitoyltransferase 1a, liver	**-3.6**	6.95E-20	2.22E-18	13.96	4.74	**upregulated**
Rps29	ribosomal protein S29	**-3.6**	6.61E-39	2.78E-37	595.98	313.83	**unchanged**
Slc46a3	solute carrier family 46, member 3	**-3.7**	3.53E-100	1.83E-98	11.63	3.95	**not significantly expressed**
Syt5	synaptotagmin V	**-3.7**	4.03E-61	1.93E-59	5.24	1.74	**not significantly expressed**
Rpl38	ribosomal protein L38	**-3.7**	3.89E-55	1.82E-53	496.75	278.37	**unchanged**
Rps28	ribosomal protein S28	**-3.9**	6.67E-18	2.00E-16	315.53	106.45	**unchanged**
Trpc6	transient receptor potential cation channel, subfamily C, member 6	**-3.9**	2.78E-67	1.35E-65	22.39	6.95	**upregulated**
Dnase2b	deoxyribonuclease II beta	**-3.9**	2.98E-59	1.42E-57	28.06	8.67	**not significantly expressed**
Tmprss11e	transmembrane protease, serine 11e	**-4.1**	5.82E-120	3.05E-118	9.73	2.93	**not significantly expressed**
Rbp3	retinol binding protein 3, interstitial	**-4.2**	1.32E-10	2.25E-09	6.69	1.97	**upregulated**
Stx11	syntaxin 11	**-4.3**	2.22E-44	9.72E-43	18.36	5.30	**not significantly expressed**

Gene ID	Gene Name	Fold Change	p-value	FDR p-value correction	WT RPKM means	Sip1cKO RPKM means	Normal expression change E10.5 to E12.5
Rpl11	ribosomal protein L11	**-4.3**	4.53E-31	1.76E-29	291.83	155.91	**unchanged**
Dpysl2	dihydropyrimidinase-like 2	**-4.4**	1.39E-79	6.95E-78	32.94	8.78	**downregulated**
Arl5c	ADP-ribosylation factor-like 5C	**-4.4**	1.44E-04	1.11E-03	3.07	0.85	**not found**
Aebp1	AE binding protein 1	**-4.5**	4.85E-219	2.61E-217	6.79	1.87	**upregulated**
Rpl19	ribosomal protein L19	**-4.5**	5.80E-10	9.20E-09	338.37	299.04	**unchanged**
Pgm5	phosphoglucomutase 5	**-4.5**	1.65E-283	8.91E-282	32.89	8.64	**upregulated**
Myo7b	myosin VIIB	**-4.5**	2.33E-35	9.46E-34	20.19	5.25	**upregulated**
Kifc3	kinesin family member C3	**-4.7**	4.80E-36	1.96E-34	4.16	1.09	**upregulated**
Faim2	Fas apoptotic inhibitory molecule 2	**-4.7**	7.62E-85	3.87E-83	4.56	1.19	**not significantly expressed**
Birc7	baculoviral IAP repeat-containing 7 (livin)	**-5.0**	1.04E-36	4.26E-35	37.34	9.16	**not significantly expressed**
Hba-x	hemoglobin X, alpha-like embryonic chain in Hba complex	**-5.0**	2.44E-04	1.81E-03	6.70	1.64	**unchanged**
Pappa	pregnancy-associated plasma protein A	**-5.0**	2.13E-40	9.09E-39	6.03	1.43	**not significantly expressed**
Rcan2	regulator of calcineurin 2	**-5.3**	2.11E-40	9.02E-39	10.15	2.36	**upregulated**
Ermap	erythroblast membrane-associated protein	**-5.3**	3.66E-305	1.99E-303	13.11	2.99	**unchanged**
Cend1	cell cycle exit and neuronal differentiation 1	**-5.8**	3.19E-29	1.21E-27	4.76	1.02	**upregulated**
Scn11a	sodium channel, voltage-gated, type XI, alpha	**-6.8**	9.47E-282	5.11E-280	7.22	1.31	**upregulated**
Rpl39	ribosomal protein L39	**-6.9**	3.24E-31	1.26E-29	489.80	259.10	**upregulated**
Ndufb4	NADH dehydrogenase (ubiquinone) 1 beta subcomplex 4	**-6.9**	1.75E-68	8.56E-67	36.87	28.71	**upregulated**
Hba-a2	hemoglobin alpha, adult chain 2	**-7.2**	6.67E-13	1.44E-11	475.53	108.94	**not found**
Rpl35a	ribosomal protein L35A	**-7.3**	6.60E-48	2.98E-46	62.48	13.72	**unchanged**
Elavl4	ELAV (embryonic lethal, abnormal vision, Drosophila)-like 4 (Hu antigen D)	**-7.4**	2.01E-97	1.04E-95	2.93	0.49	**not significantly expressed**
Cnrip1	cannabinoid receptor interacting protein 1	**-7.4**	7.37E-160	3.93E-158	5.05	0.80	**upregulated**
Ccdc109b	coiled-coil domain containing 109B	**-8.0**	7.80E-19	2.41E-17	2.36	0.35	**not significantly expressed**
Actn2	actinin alpha 2	**-9.5**	3.84E-12	7.82E-11	8.77	1.14	**not significantly expressed**
Stmn4	stathmin-like 4	**-10.0**	2.27E-65	1.09E-63	2.95	0.34	**upregulated**
mt-Atp6	mitochondrially encoded ATP synthase 6	**-10.6**	7.68E-48	3.46E-46	877.78	156.86	**not found**

Gene ID	Gene Name	Fold Change	p-value	FDR p-value correction	WT RPKM means	Sip1cKO RPKM means	Normal expression change E10.5 to E12.5
Rpl34	ribosomal protein L34	**-24.5**	7.09E-84	3.60E-82	215.28	98.65	**upregulated**
Hist1h2af	histone cluster 1, H2af	**-?**	2.83E-09	4.17E-08	4.52	0.03	**not found**

Table 2

qRT-PCR validation of EMT-related genes at E15.5. None of the genes previously linked to Sip1 are significantly altered at the RNA level when Sip1 is lost. This correlates to the RNA-Seq data.

Gene	Fold Change in Sip1 cKO†	+/- S.D.	Wild Type +/- S.D.	p-value‡
E-cadherin	-1.81	0.44/0.24	1/0.5	0.16
Vimentin	1.1	2.52/0.77	3.87/0.79	0.91
N-cadherin	-1.14	0.66/0.38	0.54/0.35	0.67
αSMA	1.17	1.03/0.55	0.51/0.34	0.63
Snail1	-1.57	0.94/0.38	1.72/0.63	0.28
Egfr	2.4	6.08/1.72	1.47/0.6	0.18
Zeb1	1.49	1.92/0.84	0.79/0.44	0.38

† calculated in Microsoft Excel, wild type set equal to 1

‡ calculated using nested ANOVA

S.D. – standard deviation

Table 3

A subset of genes, seven increasing and one decreasing in the RNA-Seq data, validated with qRT-PCR.

Gene	Fold Change in Sip1 cKO†	+/- S.D.	Wild Type +/- S.D.	p-value‡
Tnnt1[a]	29.6	23.81/13.19	0.43/0.3	0.001
Aldh1A3	44.48	67.32/26.78	6.41/0.87	0.0001
Dlk1	11.15	38.26/8.64	2.03/0.67	0.01
PlexinA2	13.78	10.44/5.94	0.6/0.37	0.000001
Dkk1	10.3	39.8/8.18	2/0.67	0.02
Dsp	5.11	9.14/3.28	2.16/0.68	0.03
Trpc6	-3.10	0.29/0.15	0.86/0.46	0.01

† calculated in Microsoft Excel, wild type set equal to 1

‡ calculated using nested ANOVA

S.D. – standard deviation

[a] n = 3, all others n = 6

Table 4

The gene promoters for a subset of differentially expressed genes, seven of which increased and one that decreased, were scanned for ZEB binding sites using TFSearch (http://www.cbrc.jp/research/db/TFSEARCH.html) using a threshold of 85.0 (default). The number of sites, position (relative to the known +1 transcription start site in the gene promoter), and sequence containing the site are reported. ZEB sites are underlined and CACCTG sites are highlighted in red, while CACCT sites are in black.

Gene	Number of Sites†	Position‡	Sequence
K8	8	-134 to -139	CCT**CACCTG**AGT
		-682 to -686	CTC**CACCT**AAAG
		-1173 to -1178	GTC**CAGGTG**GCT
		-1412 to -1417	TTG**CAGGTG**GAA
		-2050 to -2055	TTT**CACCTG**AAA
		-2067 to -2071	ACA**CACCT**AAAT
		-2410 to -2414	CCA**CACCT**TGAG
		-2433 to -2437	TCT**CACCT**TTAC
K18	1	-1215 to -1219	TTG**AGGTG**GG G G
Tnnt1	1	-1253 to -1258	GGC**CAGGTG**TGA
Aldh1A3	6	-1258 to -1263	TCT**CACCTG**CAT
		-1415 to -1419	CCA**AGGTG**GGAG
		-1872 to -1876	GGA**AGGTG**AGCC
		-2090 to -2095	ACT**CACCTG**TAA
		-2108 to -2113	ATC**CACCTG**CCT
		-2278 to -2282	TAG**CACCT**TAAT
Dlk1	4	-676 to -680	AAG**CACCT**TTAC
		-1657 to -1661	GTC**CACCT**AGAG
		-2071 to -2075	GCT**CACCT**CACT
		-2333 to -2338	GGA**CAGGTG**TGT
PlxnA2	1	-374 to -379	TCA**CAGGTG**AAG
Dkk1	3	-53 to -57	CTA**AGGTG**AGCT
		-350 to -355	AGC**CACCTG**GGC
		-2142 to -2147	CCT**CAGGTG**TGG
Dsp	3	-194 to -198	TCT**CACCT**CATA
		-634 to -638	CTG**AGGTG**TTTA
		-2413 to -2418	TGA**CAGGTG**GCA
Trpc6	3	-403 to -407	TAA**AGGTG**GGGA
		-1435 to -1439	TAG**AGGTG**AGTG
		-2246 to -2251	CAT**CACCTG**TTT

† found using TFSearch (http://www.cbrc.jp/research/db/TFSEARCH.html)

‡relative to the known +1 transcription start site in the gene promoter